1-1-2018

The Spongtang Massif in Ladakh, NW Himalaya: An Early Cretaceous record of spontaneous, intra-oceanic subduction initiation in the Neotethys

Solomon Buckman
University of Wollongong, solomon@uow.edu.au

Jonathan C. Aitchison
University of Hong Kong, University of Queensland, University of Sydney, jonathan.aitchison@sydney.edu.au

Allen Phillip Nutman
University of Wollongong, anutman@uow.edu.au

Vickie C. Bennett
Australian National University (ANU), vickie.bennett@anu.edu.au

Wanchese Saktura
University of Wollongong, wms994@uowmail.edu.au

See next page for additional authors

The Spongtang Massif in Ladakh, NW Himalaya: An Early Cretaceous record of spontaneous, intra-oceanic subduction initiation in the Neotethys

Abstract

The Spongtang Massif is a remnant of Neotethyan ocean crust emplaced onto the Indian passive margin along the Indus-Yarlung-Tsangpo Suture in the NW Himalayan region of Ladakh. The age, tectonic evolution and timing of ophiolite obduction are critical to our understanding of the mechanisms via which entire oceans are formed, consumed and partly preserved before the onset of terminal continent-continent collisions. Geochemistry of the gabbro and basaltic units suggest the presence of both MORB-type and primitive arc-related mafic rocks. Zircons extracted from the Spongtang Massif gabbros yield U-Pb (SHRIMP) ages of 136-133 Ma with initial εHfvalues of +14 to +16, indicating Early Cretaceous juvenile, depleted mantle sources devoid of contamination by older continental crust. Previously, Middle Jurassic (~177 Ma) zircon ages were obtained from gabbro and we suggest these represent MORB-type Neotethyan oceanic crust through which a younger intra-oceanic island-arc (Spong arc) developed in response to subduction initiation during the Early Cretaceous (~136 Ma). Our zircon ages are consistent with Early Cretaceous ages obtained for radiolarian cherts within the Spong Arc complex. Subduction beneath the Spong Arc continued until its collision with the northern Indian continental margin during the early Eocene. We suggest that the Spongtang Massif is equivalent to the nearby Dras island arc terrane. Intra-oceanic subduction beneath this system was possibly initiated along NNE-SSW trending transform faults in the Neotethyan Ocean, along which different ages of ocean crust was juxtaposed, thereby development of the Early Cretaceous Spong Arc is superimposed on the older Jurassic Spongtang N-MORB crust. The juvenile εHfsignature indicates the subduction system that spawned the Spong island arc was not related to the coeval Trans-Himalayan (Ladakh-Gangdese) arc that developed along the southern margin of Eurasia. The age, composition and nature of geological relationships with the underlying Indian rocks indicate the Spong Arc was a juvenile, intra-oceanic terrane that first collided with India before the onset of final continent-continent collision. Therefore, final late Eocene Neotethys closure was between the Kohistan-Ladakh (Eurasian) continental arc and the already inactive Indian + Spongtang margin.

Publication Details

Buckman, S., Aitchison, J. C., Nutman, A. P., Bennett, V. C., Saktura, W. M., Walsh, J. M. J., Kachovich, S. & Hidaka, H. (2018). The Spongtang Massif in Ladakh, NW Himalaya: An Early Cretaceous record of spontaneous, intra-oceanic subduction initiation in the Neotethys. Gondwana Research, 63 226-249.

Authors

Solomon Buckman, Jonathan C. Aitchison, Allen Phillip Nutman, Vickie C. Bennett, Wanchese Saktura, Jessica Walsh, Sarah Kachovich, and Hiroshi Hidaka

The Spongtang Massif in Ladakh, NW Himalaya: An Early Cretaceous record of spontaneous, intra-oceanic subduction initiation in the Neotethys

Solomon Buckman[1], Jonathan C. Aitchison[2], Allen Nutman[1], Vickie Bennett[3], Wanchese M. Saktura[1], Jessica Walsh[1], Sarah Kachovich[2], Hiroshi Hidaka[4]

[1]GeoQuEST Research Centre, School of Earth & Environmental Sciences, University of Wollongong

[2]School of Earth and Environmental Sciences, University of Queensland, Australia

[3]Research School of Earth Sciences, Australian National University, Canberra, ACT 0200, Australia

[4] Department of Earth and Planetary Sciences, Nagoya University, Nagoya, 464-8601, Japan

Corresponding author: Solomon Buckman, email: solomon@uow.edu.au

ABSTRACT

The Spongtang Massif is a remnant of Neotethyan ocean crust emplaced onto the Indian passive margin along the Indus-Yarlung-Tsangpo Suture in the NW Himalayan region of Ladakh. The age, tectonic evolution and timing of ophiolite obduction are critical to our

understanding of the mechanisms via which entire oceans are formed, consumed and partly preserved before the onset of terminal continent-continent collisions. Geochemistry of the gabbro and basaltic units suggest the presence of both MORB-type and primitive arc-related mafic rocks. Zircons extracted from the Spongtang Massif gabbros yield U-Pb (SHRIMP) ages of 136-133 Ma with initial ε_{Hf} values of +14 to +16, indicating Early Cretaceous juvenile, depleted mantle sources devoid of contamination by older continental crust. Previously, Middle Jurassic (~177 Ma) zircon ages were obtained from gabbro and we suggest these represent MORB-type Neotethyan oceanic crust through which a younger intra-oceanic island-arc (Spong arc) developed in response to subduction initiation during the Early Cretaceous (~136 Ma). Our zircon ages are consistent with Early Cretaceous ages obtained for radiolarian cherts within the Spong Arc complex. Subduction beneath the Spong Arc continued until its collision with the northern Indian continental margin during the early Eocene. We suggest that the Spongtang Massif is equivalent to the nearby Dras island arc terrane. Intra-oceanic subduction beneath this system was possibly initiated along NNE-SSW trending transform faults in the Neotethyan Ocean, along which different ages of ocean crust was juxtaposed, thereby development of the Early Cretaceous Spong Arc is superimposed on the older Jurassic Spongtang N-MORB crust. The juvenile ε_{Hf} signature indicates the subduction system that spawned the Spong island arc was not related to the coeval Trans-Himalayan (Ladakh-Gangdese) arc that developed along the southern margin of Eurasia. The age, composition and nature of geological relationships with the underlying Indian rocks indicates the Spong Arc was a juvenile, intra-oceanic terrane that first collided with India

before the onset of final continent-continent collision. Therefore, final late Eocene Neotethys closure was between the Kohistan-Ladakh (Eurasian) continental arc and the already inactive Indian + Spongtang margin.

1 Introduction

Debates about the age and nature of the Himalayan Orogeny centre on whether the collision was purely a single continent-continent event involving the Eurasian active margin and the Indian passive margin - see discussion by Hu et al. (2016), or involved intra-oceanic ophiolite and island-arc terranes in multiple collisions with either India or Eurasia before the onset of terminal continental collision - see discussions by Aitchison et al. (2007a). Despite the attractive simplicity of a single continental collision model (Najman et al., 2017; Wang et al., 2017), there is mounting evidence that the Indus-Yarlung-Tsangpo Suture (IYTS) extending from Tibet in the east to Pakistan in the west contains preserved fragments of juvenile ophiolite and island arc complexes that developed within a Tethyan intra-oceanic setting far from the influence of any continental crust (Aitchison et al., 2000; Corfield et al., 2001; Hébert et al., 2012; McDermid et al., 2002; Robertson and Degnan, 1994). The IYTS ophiolites typically occur as nappes thrust over the Indian margin or are disrupted into mélange within fault zones against the Eurasian fore-arc basin rocks. Importantly, the contact with Eurasian rocks is always faulted and never stratigraphically conformable (Aitchison et al., 2003) indicating they are allochthonous terranes. Paleomagnetic evidence indicate that the ophiolites formed at equatorial latitudes (Abrajevitch et al., 2005) somewhere between 1000-2500 km south of the active southern margin of Eurasia which lay between 15-25°N during Early Cretaceous time (Abrajevitch et al., 2005; Klootwijk et al., 1979; Yang et al., 2015).

The Spongtang Massif in the Zanskar mountains of Ladakh is one of the most complete fragments of Neotethyan Ocean crust preserved along the IYTS of the western Indian Himalaya (Fuchs, 1982; Gansser, 1964; Reuber, 1986; Searle, 1986). The Spong island-arc complex intruded and developed on top of this ophiolite (Pedersen et al., 2001) and was initially regarded as equivalent to the Dras Volcanics and and sedimentary equivalent Nindam Formation to the north (Fuchs, 1982). Together the ophiolite and island arc represent an important record of intra-oceanic processes operating in the Neotethyan Ocean before India collided with Eurasia to form the Himalaya (Aitchison et al., 2007a; Corfield et al., 2001). The ophiolite-arc complex collided with the northward migrating Indian continental margin at a north-dipping subduction zone resulting in emplacement of an ophiolite-arc thrust sheet onto the shallow marine, passive margin sequence – the Zanskar Supergroup (Reuber et al., 1992). This event is widely interpreted as having occurred before final closure of the Neotethyan Ocean and subsequent onset of final continent-continent collision (Aitchison et al., 2007a; Corfield et al., 2001; Pedersen et al., 2001; Reuber et al., 2015).

However, uncertainties remain regarding the age, paleogeography, tectonic setting and timing of emplacement of the Spongtang Massif. Previous U-Pb radiometric ages are limited to a U-Pb zircon ages of a diorite yielding 177 ± 1 Ma, and an andesite 88 ± 5 Ma, where the latter is associated with the Spong arc sequence overlying the ophiolite. Pedersen et al. (2001) interpreted the older age to represent that of the Neotethyan ocean crust on top of which the Spong arc developed, while the Late Cretaceous andesite age of ~88 Ma represents the minimum age of subduction initiation to form the Spong island-arc complex.

Numerous K-Ar dates by Reuber (1989) revealed two clusters of amphibole ages of 140-125 Ma and ~170 Ma (Figure 10) which approximately fits with the zircon ages, and again are consistent with a Jurassic MORB ophiolite age and a subsequent Cretaceous period of island arc igneous activity. Biostratigraphic investigations by Baxter et al. (2010) documented Early Cretaceous radiolarian faunal assemblages from red cherts amongst the Spong Arc volcanic complex, which correlates well with ophiolites along strike at Nidar, Xigaze and Zedong. Colchen et al. (1987) reported Eocene radiolarians from chert blocks in footwall mélange within the thrust zone below the ophiolite that appear to represent the youngest deep marine units of the NW Indian passive margin sequence.

Therefore, the Spongtang Massif is a critical piece of this complex tectonic puzzle. Interpretations of the tectonic setting in which it might have formed include; A) slivers of the Neotethyan Ocean accreted beneath the fore-arc of the Ladakh Arc before it was obducted onto the Indian margin (Steck, 2003); B) fore-arc basement of the Dras Arc, which evolved into the Ladakh-Kohistan Arc before final continental collision involving only a single north-dipping subduction zone (Fuchs, 1982); C) a supra-subduction zone ophiolite that evolved into the Spong Arc at the southernmost of two subduction zones between India and Asia that was partially subducted beneath the Sapi-Shergol accretionary complex of the Dras Arc before colliding with India (Groppo et al., 2016; Mahéo et al., 2006); D) oceanic basement to the intra-oceanic Spong Arc, which developed above the southernmost of three north-dipping subduction zones between India and Eurasia and collided first with India at 70 Ma, whilst the Dras-Kohistan Arc collided with the Trans-Himalayan Arc between 102-75 Ma before it

evolved into the continental Ladakh (Trans-Himalayan) Arc prior to final continental collision at 55 Ma (Corfield et al., 2001). We address aspects of the age and origin of the Spongtang Massif using an integraded program of field geology, whole-rock geochemistry and U-Pb and Lu/Hf analysis of zircons extracted from gabbro and leucogabbro samples, to assess the influence any continental crustal material had during generation of melts during ophiolite-arc formation.

2 Geological Setting

2.1 Spongtang Massif

The Spongtang Massif crops out as an isolated klippe situated between 4000-6000 m elevation near the village of Photoksar about 30 km south of the Indus Suture (Figure 2). This ophiolite has attracted the attention of geologists for over a century (La Touche, 1888; Lydekker, 1880; Lydekker, 1883; MacMahon, 1901) and was the focus of several mapping expeditions in the 1980s, which provided detailed geological maps (Bassoullet et al., 1980; Colchen et al., 1987; Fuchs, 1979, 1982; Honegger et al., 1982; Kelemen and Sonnenfeld, 1983; Reibel and Reuber, 1982; Reuber, 1986; Reuber et al., 1992; Reuber et al., 2015; Reuber et al., 1989).

The Spongtang Massif displays all elements of a formerly complete “Penrose-style” ophiolite stratigraphy, albeit significantly disrupted by faulting. Early studies concentrated on the mantle peridotites and lower crustal cumulates (Reibel and Reuber, 1982) in an attempt to identify fabrics that might indicate stress regimes associated with a spreading ridge (Reuber, 1986). Detailed mapping identified an upper lherzolite unit rich in pyroxene structurally

overlying a more depleted harzburgite unit (Reuber et al., 1992). Lower crustal cumulate rocks include wehrlite, pyroxenite and gabbro. They crop out along the eastern side of the Photang valley and west side of Marling chu valley (Figure 2), where they are intruded by medium-grained basaltic dykes (Corfield et al., 2001; Reuber et al., 1992; Reuber et al., 2015). Minor gabbro cumulates occur within the lower unit on the east side of Photang Kangri and along the Marling Valley section (Reuber et al., 1992). Gabbro also occurs within the dominantly basaltic-andesite volcanic west side of Photang Kangri and along Photoksar Valley where our samples were collected. Corfield et al. (2001) observed two generations of dykes; 1) coarse-grained pegmatitic gabbroic dykes intruding the harzburgites, and 2) medium-grained basaltic dykes indicating at least two stages of mantle melt generation. Dunite bodies also intrude both peridotite units. Corfield et al. (2001) reported rare plagiogranites within the mantle sequence but were not successful in extracting zircons from these samples. We collected gabbro, leucogabbro and pegmatitic gabbro from the Photong Valley for zircon extraction. Two samples gave low yields of small zircons amenable to dating using the Sensitive High-Resolution Ion Microprobe (SHRIMP) at Hiroshima University.

Partial remnants of a once extensive ophiolite thrust sheet over the northern Indian margin are locally preserved along the Indus-Yarlung-Tsangpo Suture Zone. The nearest complete ophiolite sequence to Spongtang Massif is the Nidar ophiolite (~140 Ma) about 120 km east (Ahmad et al., 2008; Mahéo et al., 2004; Zyabrev et al., 2008). Further east, the Indus Suture is offset dextrally by the Karakorum Fault but correlatives are found in Tibet as

part of the Dazhuqu and Zedong terranes (Aitchison et al., 2000). Individually, these include ophiolites recorded at Jungbwa (Miller et al., 2003), Saga and Sangsang (Bédard et al., 2009), Xigaze (Dubois-Cote et al., 2005; Dupuis et al., 2005; Girardeau et al., 1984; Girardeau et al., 1985a; Nicolas et al., 1981; Wang et al., 1987), Dazhuqu (Girardeau et al., 1985b; Xia et al., 2003), Zedong (Aitchison et al., 2007b; McDermid et al., 2002) and Luobusa (Zhou et al., 1996). Correlatives to the west in Pakistan include Bela (Sarwar, 1992; Zaigham and Mallick, 2000), Muslim Bagh (Moores et al., 1980) and Waziristan ophiolites (Jan et al., 1985). The magmatic ages of these ophiolites vary from Jurassic to Cretaceous (Fig. 1).

2.2 Indian margin – Zanskar Group

The Permian-Eocene northern Indian passive margin platform sequence or "Zanskar Supergroup" over which the ophiolite klippe is thrust has been described in detail previously (Fuchs, 1982; Gaetani and Garzanti, 1991; Garzanti et al., 1987). Mud-matrix mélange directly underlies the ophiolite klippe (Reuber et al., 1992; Reuber et al., 2015). Collectively, the large and varied blocks within a mud-matrix mélange are associated with the Lamayaru Complex (Brookfield and Andrews-Speed, 1984). Robertson and Degnan (1993) interpret the Lamayuru Complex as outer shelf to slope deposits of the Indian margin. This margin experienced pulses of extension and drastic collapse of the carbonate platform edge during the mid-Jurassic as a convergent plate boundary approached resulting in submarine channels being filled with a mixture of shallow water limestone olistoliths and deep marine cherts and clastics. While the Lamayaru Complex was initially deposited as a passive margin succession, it displays scaly mud-matrix and block in matrix textures characteristic of

overpressuring due to tectonic crustal loading. Mud-matrix mélange is commonly associated with collision complexes involving obduction of an island-arc complex onto a passive continental margin, for example, the Lichi mélange in Taiwan (Huang et al., 2008). Such mélange within the Lamayaru Complex is possibly a correlative of the Yamdrok mélange in Tibet (Liu and Aitchison, 2002).

The youngest marine shales deposited on the Indian passive margin are the Lower Eocene Chulung la Formation and Kong slates which structurally underlie the Spongtang Massif thrust sheet further south at Dibling (Fuchs, 1982; Fuchs and Willems, 1990). Najman et al. (2017) undertook detrital zircon studies of the Kong and Chulung la formations and reported a youngest detrital zircon age of ~53 Ma thereby establishing the maximum depositional age. Both formations show a strong Mesozoic to Cenozoic distribution (55-70 Ma and 90-100 Ma) and rare Precambrian zircons. Najman et al. (2017) interpret zircon grains older than ~130 Ma to have been sourced from southern Eurasian margin because of the presence of two ~140 Ma grains of positive εHf value while older Precambrian grains are display mostly negative ε_{Hf} values and therefore sourced from (Gondwanan) Lhasa terrane. Zircons less than 115 Ma display mostly positive ε_{Hf} values that drop to negative values for the youngest grains which they suggest is consistent with a Kohistan-Ladakh-Gangdese Arc source. However, we suggest that the age and ε_{Hf} values of the Kong and Chulung la formations are consistent with derivation from the structurally overlying Spong and Dras island arc immediately overlying and to the north of these units. The intra-oceanic Spong and Dras island arc would have been active until its collision with India during the early Eocene.

The trend towards negative ε_{Hf} values in younger grains is consistent with subduction of continental margin sediment from India beneath the Dras Arc just prior to arc-continent collision along with an influx of Indian-derived older Precambrian zircons. The two ~140 Ma zircons with positive εHf values are consistent with zircons from the Spongtang Massif presented here.

Reuber et al. (2015) suggested that the youngest sediments of the Indian passive margin sequence must constrain the maximum age of obduction and therefore structural relationships between the lower Eocene Chulung la Formation and Kong Slates that tectonically underlie the Spongtang Massif constrain ophiolite obduction to post- early Eocene. This is consistent with tectonic reconstructions that place northern India at about 10°N (Aitchison et al., 2007a; Dewey et al., 1989; Molnar and Tapponnier, 1975) and at least 1000 km south of Eurasia at 45 Ma when the Ladakh Arc on the southern margin of Eurasia was at 23°N (Klootwijk et al., 1979). However, Corfield et al. (1999) proposed that obduction of the Spongtang Massif must have occurred during the Late Cretaceous based on their interpretation that an allochthonous thrust sheet of continental slope deposits is truncated by uppermost Cretaceous to lower Eocene deposits and are therefore post-collisional. They invoke a later phase of thrust faulting following collision of India with Eurasia to explain why the Spongtang Massif is thrust over these lower Eocene deposits.

2.3 Dras Volcanics and Nindam Formation

The Dras Volcanics and correlative volcaniclastic rocks of the Nindam Formation crop out extensively to the east of Kargil and represent a poorly understood package of

island-arc volcanic rocks and immature volcaniclastic rocks faulted between Eurasian margin derived sediments (Tar and Indus groups) to the north and the Indian margin (Zanskar Group) to the south (Clift et al., 2000; Fuchs, 1982; Reuber, 1989; Robertson and Degnan, 1994). They were originally described and referred to as the Zanskar flysch by Sterne (1979), which is overlain by the Chilling Formation (Fuchs, 1986). Some interpret the Nindam Formation as a continuation of the Indus Molasse sequence (Tar Group) suggesting that together they formed in a fore-arc basin that flanked the Ladakh Arc to the north (Garzanti and Van Haver, 1988; Henderson et al., 2010; Henderson et al., 2011). However, contacts between the two units are faulted and locally marked by extensive mélange development, such as the Mongyu mélange located between Khaltse and Mongyu villages (Fuchs, 1982). Detailed petrographic and lithofacies analysis of the Dras-Nindam units by Robertson and Degnan (1994) indicates that the Nindam Formation differs markedly from the Andean-type fore-arc succession of the Trans-Himalaya (Ladakh Block) or Tar Group immediately to the north of the Mongyu mélange (Figure 2). Sandstones from the Albian-Aptian Khalsi limestone (Tar Group) north of the Mongyu mélange are dominated by metamorphic quartz and minerals such as hornblende that are rare or absent in the coeval Nindam Formation. The Paleocene Trans-Himalaya fore-arc basin succession overlying the Khalsi Limestone contains thick, channelized conglomerate units containing abundant granite/rhyolite clasts while coeval sections of the Nindam Formation formed in deep marine, hemipelagic environments and are dominated by immature volcaniclastic sedimentary and pyroclastic rocks. On the basis of these fundamental differences, Robertson and Degnan (1994) interpret the Dras Volcanics

and Nindam Formation to have formed in an intra-oceanic island-arc setting, most likely in a fore-arc basin setting assuming northward subduction. Differences between the Dras and Ladakh arcs are further highlighted by distinct geochemical differences of volcanic rocks of the island arc Dras Volcanics and continental arc Khardung Volcanics respectively as reported by Clift et al. (2002a).

2.4 Chilling Formation

The Chilling Formation was first described and named by Sterne (1979) as a sequence of red-purple-green siltstones and mass-flow volcaniclastic conglomerates (Skiu conglomerate) that overlie the Dras-Nindam unit (Zanskar flysch). Clasts within conglomerates of the Chilling Formation consists of ophiolite-derived peridotite, gabbro, basalt, chert and volcaniclastic rocks similar to lithologies within the adjacent Dras ophiolitic mélange. They also include nummulitic limestone and quartzite clasts derived from the Indian Zanskar Group and Lamayaru Complex. Sterne (1979) considered the Chilling Formation to be an outlier equivalent to the Spongtang Massif but Fuchs (1986) renamed it the “Chilling Molasse” and interpreted it as the youngest portion of the Dras unit. Brookfield and Andrews-Speed (1984) were unable to correlate this unit and regarded it as unassigned molasse. Searle et al. (1990b) regarded this unit as equivalent to both the Chogdo and Nindam formations, while others assigned it to the Chogdo and Khalsi formations (Clift et al., 2001, 2002). Henderson et al. (2011) disagreed with previous correlations between the Chilling and Chogdo formations based on the radically different geochemical and detrital zircon signatures of these units. More recently, Baxter et al. (2016) presented chrome spinel

evidence from the Chilling Formation and concluded that the ultramafic clasts present were derived from the Spongtang Massif. The Chilling Formation consists entirely of ophiolite and Indian-derived detritus and this is reflected in detrital zircon populations which show little or no Eurasian source. The youngest reported zircon population is ~159 Ma which Henderson et al. (2011) suggest is derived from the Indus ophiolites such as Spongtang. In contrast, the Chogdo Formation is dominated by 40-85 Ma zircons derived from the Ladakh Arc. Chilling Formation shales have high Cr and Ni concentrations approaching values within the ophiolite source rocks while Chogdo Formation has low concentrations of Cr and Ni and is dominated by felsic volcanic and intrusive clasts. Finally, the red conglomerates and shales typical of the Chilling Formation are not present in the Chogdo Formation and on the weight of this evidence Henderson et al. (2011) preferred not to correlate the two formations.

In Tibet, obduction of the ophiolite-arc complexes with the Indian margin is marked by the presence of a distinct conglomerate unit – the Luiqu conglomerate (Davis et al., 2004) which is probably equivalent to the Chilling Formation in Ladakh (Baxter et al., 2016). Deposition of this distinct ophiolite + Indian continent derived conglomerate marks the onset of arc-continent collision at ~55 Ma. The final continent-continent collision is marked by the deposition of the Lower Miocene (~34 Ma) Gangrinboche conglomerates in Tibet (Aitchison et al., 2002) and the Indus Group (molasse) in Ladakh (Henderson et al., 2010).

2.5 Ladakh Batholith (Trans-Himalayan Batholith)

The Ladakh Batholith occurs as a WNW–ESE trending linear belt, spanning an area approximately 600 km long and 30–80 km wide (Singh et al., 2007) and is bound by the

Indus Suture Zone to the south and the Shyok Suture Zone along its northern margin (Frank et al., 1977). The Ladakh Arc is composed of a calc-alkaline intrusive suite, ranging in composition from gabbroic to granitic (Honegger et al., 1982; Singh et al., 2007), and a carapace of andesitic to rhyolitic eruptive rocks assigned to the Khardung Volcanics (Dunlap and Wysoczanski, 2002). Leucogranite intrusions (Reichardt et al., 2010) and andesitic dykes (Heri et al., 2015) are also reported. Locally, the Ladakh Batholith intrudes the Jurassic?-Cretaceous Shyok Volcanics (Borneman et al., 2015) along its northern margin, evident by the numerous basaltic xenoliths within granitoids (Kumar et al., 2016) and minor Jurassic sedimentary rocks of the Tsoltak Formation (Ehiro et al., 2007; Reuber, 1990). Vadlamani and Guha (2002) reported Miocene (~24 Ma) ultrapotassic dykes that intruded the Ladakh Arc and correlated these with post-collisional intrusions in Tibet (Miller et al., 1999; Ravikant, 2006).

The Ladakh Batholith, together with the Kohistan Batholith to the north-west and the Gangdese Batholith to the east, collectively forms the Trans-Himalaya Batholith, which has yielded diachronous magmatic crystallization ages between 103 Ma to 41 Ma, younging to the east (Ravikant et al., 2009; Reichardt et al., 2010; Shellnutt et al., 2014; Weinberg and Dunlap, 2000). The Gangdese Batholith displays discrete pulses of magmatism at ~205–152, ~109–80, ~65–41 Ma (Ji et al., 2009) while the Ladakh Batholith displays distinct magmatic pulses between 66-41 and 85-75 Ma (White et al., 2011) and a smaller 90-110 Ma peak recorded in detrital zircon studies of the Indus Group (Henderson et al., 2010) but no evidence of older pulses. Alternatively, Bouilhol et al. (2013) suggest that the Ladakh-

Kohistan Batholith is not part of the Trans-Himalayan Batholith but a separate intraoceanic island arc (Bouilhol et al., 2014 and others) generated on a separate subduction system to the continuous Gangdese-Karakoram continental arc developing on the southern margin of Eurasia. They include the Spongtang Massif and Dras Arc as different sections of a single arc that includes the Kohistan-Ladakh batholith. While the Kohistan-Ladakh batholiths do display island arc characteristics it is difficult to reconcile the need to separate them from the Gandese Batholith which has the same age range and juvenile ε_{Hf} values and is continuous along strike when displacement across the Karakoram Fault (~150 km) is taken into consideration. The Karakoram Batholith displays more similarities in age and composition (Rex et al., 1988; Searle et al., 1990a; Searle and Tirrul, 1991; Searle et al., 1998) with Mesozoic granites along the Bangong-Nujiang Suture between Qiangtang and Lhasa blocks in Tibet (Liu et al., 2014). Rolland (2002) suggested that the relationship between the Kohistan, Ladakh and Gangdese batholiths might be transitional from purely island arc in the west to continental arc in the east and we suspect it was similar to the modern day Aleutian Arc. In Tibet, the youngest age of the equivalent Gangdese Batholith is ~41 Ma (Ji et al., 2009) but detrital zircon studies indicate that magmatic activity may be as young as 37 Ma (Aitchison et al., 2011), suggesting that northward subduction beneath the southern margin of Eurasia (Lhasa Block) continued until late Eocene time and continent-continent collision may not have started until at least after ~37 Ma.

2.6 Tar Group – Ladakh Fore-arc Basin

The oldest units within the Indus Basin are the Albian-lower Eocene predominantly marine sequence commonly referred to as the Tar Group (Henderson et al., 2010; Searle et al., 1990b; Sinclair and Jaffey, 2001) or Indus Flysch (Fuchs, 1979, 1981). The Tar Group consists of deep marine limestones and turbidites (Khalsi limestone), overlain by Late Cretaceous to Paleocene marine marls, mass flow deposits and shales of the Jurutze Formation. The Tar Group is interpreted as the marine fore-arc basin to the Ladakh Arc, which developed slightly outboard of southern Eurasia prior to the onset of continental collision (Clift et al., 2002b; Garzanti and Van Haver, 1988; Sinclair and Jaffey, 2001; Steck et al., 1993). In Tibet, this fore-arc sequence is well recognized as the Xigaze Group (Aitchison et al., 2011; Dürr, 1996; Einsele et al., 1994; Wang et al., 1999). Henderson et al. (2010) collectively refer to the Tar Group and the conformably overlying, post-early Eocene Indus Group as Indus Basin sedimentary rocks.

The basal contact of the Tar Group has been interpreted differently by different authors. Searle et al. (1990b) considered the oldest units of the Tar Group as disconformable cover to the Cretaceous Nindam Formation. However, our geological mapping indicates that the oldest unit in the Tar Group, the Khaltsi Limestone, is always in fault contact with the Dras-Nindam unit to the south with the contact marked by distinctive serpentinite-matrix mélange (Mongyu mélange). This melange includes blocks of peridotite, gabbro, basalt and volcaniclastic rocks. Clift et al., (2000) assigned the lowermost parts of the Indus Group to the Chogdo Formation and interpreted this unit as a correlative of the Chilling Formation,

which they considered, unconformably overlies the Nindam Formation, Lamayaru Complex and Tar Group and contains ophiolitic clasts. This led Clift et al. (2002b) to infer that the age of the Chogdo Formation might constrain the maximum age of collision. Based on this reasoning, they suggested that the well-established Early Eocene (Ypresian) age of the Nummulitic limestone, which overlies the Chogdo Formation, indicates continent-continent collision must have occurred prior to 49 Ma. However, more detailed stratigraphic and provenance studies by Henderson et al. (2011) exclude any possibility that the Chogdo and Chilling formations might be correlatives thus they cannot be used to constrain the timing of collision. The Chogdo Formation is dominated by felsic igneous clasts derived from the Ladakh Arc whereas the Chilling Formation is dominated by ophiolitic and quartzite-limestone clasts of Indian and ophiolite provenance but no Eurasian influence. The Chilling Formation formed on the Indian Plate as Indus ophiolites were being obducted, whereas the Chogdo Formation accumulated in a fore-arc basin associated with the Ladakh Arc on the southern Eurasian margin.

2.7 Post-collisional Indus Group (molasse)

Fore-arc basin sedimentary rocks of the Tar Group are succeeded by post-early Eocene to Miocene molasse of the Indus Group (Baud et al., 1982; Henderson et al., 2010; Searle et al., 1990b; Sinclair and Jaffey, 2001; Tewari, 1964). These high-energy, fluvial conglomerates and sandstones mark the onset of the India-Eurasia continental collision and intra-montane basin development. In places, the Indus Group is deposited unconformably on granites of the Ladakh Batholith (Garzanti and Van Haver, 1988; Searle et al., 1997)

indicating considerable uplift and erosion of the Ladakh Arc prior to deposition. Detrital zircon studies of the Indus Group by Henderson et al. (2011) reveals that the youngest detrital zircon population is 41 Ma within sandstones of the upper Nimu Formation suggesting that calc-alkaline magmatism within the Ladakh Arc continued until at least 41 Ma. This is significant because the age of the youngest arc-related, calc-alkaline magmatic rocks possibly constrains the timing of terminal continental collision (Searle et al., 1988). In Tibet, detrital, arc-derived zircons as young as 37 Ma from the upper Oligocene post-collisional Gangrinboche conglomerates (Aitchison et al., 2011) indicate that subduction-related convergent margin magmatism continued along the southern margin of Eurasia until at least the Late Eocene before final collision of India and Eurasia. The Indus Group sedimentary rocks have experienced substantial NE-SW directed compression resulting in km-scale folds and some refolded folds (Henderson et al., 2010; Searle et al., 1990b). This intense deformation and faulting complicates resolution of stratigraphic relations in Ladakh.

3 3. Analytical methods

Standard methods were employed for whole-rock geochemistry including X-ray fluorescence (XRF) for major and trace elements at University of Wollongong (Table 1) and inductively coupled plasma mass spectrometry (ICP-MS) for rare-earth elements (REE) at Australian Laboratory Services in Brisbane (Table 1). Methods are described in detail in Appendix 1. U-Pb zircon geochronology (Table 2) was undertaken using the SHRIMP at Hiroshima University and detailed methodology is given in Appendix 2. Zircon Lu-Hf

isotope analysis (Table 3) was undertaken using LA-ICP-MS at the Australian National University (ANU) (Appendix 3). Method description along with the complete data for the 6 reference zircons (FC-1 Plesovic, QGNG, Monastery, Mud Tank and R-33) analysed throughout the analytical session are provided in Appendix 3).

4 Results

4.1 Field relations and petrography

4.1.1 Gabbro

Gabbros collected from Photang valley range in composition and texture from layered olivine-hornblende gabbro (SBST19 – Figure 3 and 4) to isotropic hornblende gabbro, leucogabbro and pegmatitic hornblende gabbro dykes (Figure 4). The amphibole-rich gabbro-diorite dykes intrude both the mantle (ultramafic) and mafic volcanic sequences. Leucocratic gabbros are also incorporated as blocks in the basal serpentinite mélange. Leucogabbro sample SBST05 was collected from an outcrop near the base of the klippe along Photoksar valley. The leucogabbro intrudes a larger serpentinised peridotite block and is incorporated into the highly disrupted, basal serpentinite-matrix mélange (Figure 3). Other samples for this study were collected from the upper reaches of the Photang valley (Figure 2). Thin (1-3 m) dykes and sills of pegmatitic, amphibole-rich gabbro intrude the massive gabbro and peridotites (Figure 3). The abundance of amphibole as part of the igneous assemblage in these rocks indicates a hydrous magma.

Thin-section petrography of gabbro samples shows that unaltered, euhedral hornblende phenocrysts are the dominant mineral phase in most samples including the more mafic olivine-hornblende gabbro (SBST19 - Figure 4A). Igneous hornblende occurs as large euhedral phenocrysts aligned with cumulate layering and displays strong green to light brown pleochroism typical of magmatic hornblende. Isotropic gabbros contain randomly orientated hornblende, pyroxene and plagioclase phenocrysts. Some leucogabbro samples contain kaersutite amphibole identified by its deep yellow/orange to brown pleochroism. The occurrence of rare poikilitic olivine within clinopyroxene phenocrysts is interpreted to demonstrate an early stage of anhydrous, tholeiitic crystallization prior to water saturation (Figure 4A). Clinopyroxene is present in the more mafic gabbros but is always subordinate to hornblende and commonly rimmed by hornblende. Early stage, subhedral plagioclase phenocrysts are present in most samples but are ubiquitously altered to a semi-opaque, yellow-brown mixture of fine-grained albite-sericite-epidote-calcite-quartz (Figure 4A-H). Accessory igneous minerals include late stage magnetite rimming hornblende, rutile, quartz, ilmenite, zircon, and apatite. Some of the more felsic leucogabbros contain needles of metamorphic actinolite (Figure 4F) rimming the igneous hornblende. Selective alteration of plagioclase is pronounced such that Carlsbad twinning is rarely observed and distinctly contrasts with neighbouring, unaltered hornblende and clinopyroxene (Figure 4D). This suggests that crystallization initially followed a typical anhydrous path of olivine-anorthite-clinopyroxene before water saturation of the magma resulted in hornblende crystallization and pervasive alteration of earlier crystallized anorthite. Alternatively, the original anhydrous

gabbro may have undergone re-melting at a later stage to generate a hydrous hornblende gabbro. Small lenses and veins of fresh, interlocking quartz, albite and microcline occur in leucogabbro sample SBST16 (Figure 4D-F) and in the pegmatitic gabbro sample SBST20 (Figure 4G-H). These do not appear to be a result of high temperature alteration or metamorphism but the partial resorption of the highly altered, early plagioclase may represent small patches of felsic partial melt extracted from the surrounding gabbros.

4.2 Whole-rock geochemistry

Gabbros have a narrow SiO_2 range between 46-54% (Table 1, Figure 5). The most mafic layered cumulate sample (SBST19) has relatively high MgO (11%), Mg# (67), CaO (13.8%), Cr (960 ppm) and Ni (193 ppm), which is reflected by the presence of normative olivine and clinopyroxene as well as abundant hornblende. This sample is geochemically distinct from the other more evolved gabbro and leucogabbro samples, which have lower MgO values (4.38-8.36%), Mg# (31-43), CaO (6.7-9.9%), Cr (50-390 ppm) and Ni (20-136 ppm). Most of the gabbros are characterized by low K_2O (0.18-0.84%) and moderate TiO_2 (0.35-1.25%), Fe_2O_3 (6-12%), P_2O_5 (0.05-0.15% but generally <0.08), Zr (18-83ppm), Nb (0.2-3ppm), Y (6.5-25 ppm). Spongtang Massif gabbros initially follow a trend showing early iron enrichment (Figure 5C) due to early olivine and pyroxene crystallization until about 52% SiO_2 (MgO 12-5%) followed by rapid drop in iron content as hornblende dominates the crystallization process along with accessory magnetite. Both Sr (resident in plagioclase) and Al_2O_3 display flat trends when plotted against MgO indicating that plagioclase was not being

crystallized following its early crystallization with olivine and clinopyroxene. This matches petrographic descriptions, which show highly altered plagioclase enveloped in fresh hornblende in most samples (Figure 4A-E). Fractionation trends involving iron enrichment are typical of ophiolites unrelated to subduction in which anhydrous crystallization of water undersaturated magmas is the norm (Dilek and Furnes, 2011; Miyashiro, 1975). However, the hornblende-rich gabbros from the Spongtang Massif suggest that early crystallization of unsaturated tholeiitic magma shifted to crystallization of water saturated, hydrous melts and is more consistent with the combination of calc-alkaline and tholeiitic magmas found in island arc environments (Miyashiro, 1973; Pearce and Robinson, 2010).

Chondrite normalized REE patterns for the Spongtang gabbro are generally flat with a slight depletion in the light rare earth elements (LREE) compared to the flat, and slightly more elevated patterns of the basalts (Figure 6A). An exception is a pronounced positive Ce anomaly for a gabbro (SBST17) and one basalt sample (SBST08). While negative Ce anomalies reflect the subduction of pelagic sediments and seawater alteration (Hole et al., 1984), positive Ce anomalies are more likely to be associated with the highly oxidizing, fluid-rich nature of the gabbroic melts that formed in a supra-subduction zone setting and had fractionated past silica-saturation and started crystallizing zircon, which unlike most minerals strongly partitions Ce^{4+} but not Ce^{3+} (Ballard et al., 2002). Eu anomalies do not occur in any samples indicating that plagioclase was not fractionated during magmatic crystallization (Pallister and Knight, 1981). Middle to heavy REE patterns are flat for gabbros and basalts reflecting early olivine, plagioclase and pyroxene crystallization while the slight, relative

depletion in LREE is consistent with a depleted mantle source and/or late stage crystallization of hornblende, which does not retain LREE (Kocak et al., 2005). High-field strength (HFS) element (Hf, Zr, Ti, Nb and Ta) concentrations are low to moderate, reflecting a slight depletion associated with subduction related magmas (Pearce, 1975). Both gabbro and basalt samples display negative Nb-Ta anomalies (Figure 6F) due to the compatible and immobile nature of these elements in oxidizing supra-subduction zone conditions (Pearce, 2008). However, there is a distinct enrichment of mobile and incompatible large ion lithophile (LIL) elements (Figure 6F) typical of subduction-related magmas (Pearce and Robinson, 2010).

Tectonic discrimination plots (Pearce, 1982; Pearce, 2008; Pearce and Cann, 1973; Shervais, 1982) show basalts of the Spongtang Massif generally plot in the N-MORB field. However, basaltic andesites of the Spong Arc plot in the island arc field (Figure 6A-D). Most Photang Valley gabbro samples plot in the island arc field with a few exceptions plotting in the N-MORB field. The Th/Yb-Nb/Yb plot of Pearce (2008) clearly demonstrates the N-MORB affinities of the Spongtang Massif basalts and the departure to the island arc field for the younger Spong Arc samples (Figure 6C). The gabbros collected in this study show a gradual but clear displacement from the basalts falling on the MORB-OIB array towards the island arc field (Figure 6C). Increasing Th/Yb ratio reflects the gradual increase of subducted sediments shed off the evolving island arc and recycled back into the gabbro melt while the slight decrease in Nb/Yb ratio reflects the conservative, immobile and compatible nature of Nb in highly oxidized environments such as subduction zones (Pearce, 2008). The discrimination plots of V/Ti*1000 (Shervais, 1982), Ti/Zr (Pearce and Cann, 1973) and Th-

Ti-Zr/117 (Wood, 1980) all show a clear discrimination of the N-MORB basalts from the island arc gabbros (Figure 6A-D). This supports field observations in which gabbro dykes and sills intruded the volcanic rocks and mantle peridotites, and suggests there was a second stage of magmatism associated with island arc development that was superimposed on pre-existing N-MORB type crust or MORB-like fore-arc crust associated with the earliest phase of subduction, for example, Izu-Bonin-Marianas arc basement (Ishizuka et al., 2018).

4.3 SHRIMP U-Pb zircon results

Approximately 1-2 kg of both gabbro samples SBST05 and -12 gave zircon yields of ~50 (50-100 μm) and ~100 (100-250 μm) grains respectively. Sample SBST05 zircons are cloudy yellow, prismatic grains and fragments, in which oscillatory zoning is widely disrupted by recrystallisation (Figure 7). SBST12 zircons are translucent to pale yellow, euhedral, oscillatory zoned and of equant to stubby prismatic habit (Figure 7). The small size of zircon grains in sample SBST05 considerably reduced the choice of sites for analysis. Zircons from sample SBST12 are markedly larger, which afforded a greater choice of sites for analysis.

For gabbro sample SBST12, 12 analyses were undertaken on 12 grains. Sites from CL images indicating recrystallisation were avoided (Figure 7, Table 2). The chosen sites have U content of 188-583 p.p.m., with elevated Th/U of 0.55-1.55. These elevated Th/U values are typical of zircons crystallised from intermediate to gabbroic magmas (e.g., Paces and Miller 1993). Uncorrected for minor amounts of common Pb, all sites yield close to concordant U-

Pb ages, with all having indistinguishable $^{238}U/^{206}Pb$, but with small dispersion in $^{207}Pb/^{206}Pb$ (Figure 8). Those with the highest $^{207}Pb/^{206}Pb$ show marginally higher amounts of common Pb (Table 2). After correction for common Pb by the '207' method (Compston et al., 1984), all analyses yield a weighted mean $^{206}Pb/^{238}U$ age of 135.9±1.2 Ma (95% confidence, MSWD=1.05).

For gabbro sample SBST05, only four analyses were completed due to the small and partially metamict state of the grains (Table 2). Other analyses were attempted but aborted, due to the small size of grains and much higher levels of common Pb being present (judged from high ^{204}Pb count rates in the first peak-hop cycle). The SBST05 zircons have considerably higher U content (846-1488 ppm), with very high Th/U (2.39-7.09). These grains are interpreted to be magmatic in origin, formed from U-enriched melt at the last stage of crystallization of the intermediate-gabbroic magma. The completed analyses have higher common Pb content than those in sample SBST12, and uncorrected for common Pb form a slightly discordant population with real dispersion in $^{238}U/^{206}Pb$ and $^{207}Pb/^{206}Pb$ (Figure 8). Analysis 4.1 with high U and high common Pb gives an apparently younger $^{206}Pb/^{238}U$ age than the other sites and might have lost some radiogenic Pb in a recent event. After correction for common Pb by the '207' method, analyses 1.1, 2.1 and 3.1 give a weighted mean $^{206}Pb/^{238}U$ age 133.3±9.1 Ma (95% confidence, MSWD=4.1). Within its larger error (due to the lesser number of analyses), this is indistinguishable from the age of the SBST12 zircons. These ages indicate magmatic crystallization of samples SBST05 and SBST12 at 136-133 Ma (Early Cretaceous; Hauterivian-Valanginian).

4.4 LA-ICP-MS Lu-Hf results

Due to the small size of the SBST05 zircons, LA-MC-ICP-MS analyses were not attempted, and only SBST12 grains were analyzed (Table 3). Eleven analyses were undertaken over SHRIMP U-Pb analysis sites, together with an additional seven analyses on sites free of evidence of recrystallization from CL images, but without prior U-Pb analysis. Present day ε_{Hf} ranges from +12.1 to +14.9 (all ε_{Hf} values are calculated using a present day CHUR composition of $^{176}Hf/^{177}Hf = 0.282785$ and $^{176}Lu/^{177}Hf = 0.0336$; Bouvier et al., 2008) with minor spread beyond analytical error, whereas ε_{Hf} at 136 Ma – the time of igneous crystallisation of the zircons, ranges from +14.3 to +18.9 with a weighted mean value of 16.0±0.5 (95% confidence). These values are equal to estimates for depleted MORB source mantle at that time. Hence, there is no evidence of any crustal contamination in the mantle source from subducted older crustal materials or through mixing in the arc roots with older crust, as is seen in most arc suites (as summarized by Jones et al., 2015).

5 DISCUSSION

5.1 Geochronology and Hf isotope signatures

Heitz (1986) first reported a whole-rock K-Ar age of 140 ± 15 Ma for Spongtang Massif basalts. Reuber et al. (1989) obtained several K-Ar ages from basic dykes collected from the Spongtang Massif. They yielded two clusters of amphibole ages - the first between 140-125 Ma which they interpreted as the age of dyke intrusions and the second at about 170

Ma which they interpreted as the minimum age of formation of the ophiolite. It should be noted that most of the Spongtang Massif rocks have been metamorphosed to sub-greenschist facies and consequently K-Ar dates are unlikely to be reliable given the mobility of K and Ar during metamorphism. Mahéo et al. (2004) undertook ^{40}Ar-^{39}Ar dating on amphiboles of the Spongtang Massif, which yielded ages between 130-110 Ma. Pedersen et al. (2001) reported a TIMS single zircon age of a diorite from Spongtang Massif at 177 ± 1 Ma, which they interpreted to be the age of the ophiolite basement before development of the Spong Arc. Whether this Jurassic age represents the original MORB ocean crust or an early phase of supra-subduction zone ophiolite-arc development is difficult to determine. This Jurassic age is similar to the Zedong terrane in Tibet (McDermid et al., 2002) but older than most other ophiolite fragments along the IYTS, such as Xigaze at ~126 Ma (Aitchison et al., 2003; Malpas et al., 2003). Pedersen et al. (2001) also reported that zircons from andesitic rocks of the overlying Spong Arc volcaniclastic sequence yielded an age of 88 ± 5 Ma, which they interpreted to constrain the minimum age of subduction initiation beneath the Spongtang Massif. Our samples are of gabbros with arc-like whole rock geochemistry that yielded magmatic zircons of 136 Ma and 133 Ma. The Cretaceous (~136 Ma) gabbros, which intrude both the mantle and volcanic ophiolite sections have a distinct supra-subduction geochemical signature (Figure 6) and possibly signify intra-oceanic subduction initiation and fore-arc spreading in ~177 Ma oceanic crust, which led to the development of the Spong island-arc during the Cretaceous. The Hf isotopic data obtained from SBST12 with initial ε_{Hf} of +14.3 to +18.9 show that this sample formed in a setting free of detectable contamination by older

continental crust (Figure 9). This shows there was neither distally or locally derived continental trench sediment nor extended older continental crust in the roots of the arc.

The Cretaceous U-Pb zircon age of ~136 Ma we report here differs from previous Jurassic U-Pb age of ~177 Ma of Pedersen et al. (2001) but is similar to the Ar-Ar ages provided by Mahéo et al. (2004). We suggest this older Jurassic ages relates to fragments of Neotethyan, MORB-like, oceanic crust of the Spongtang ophiolite, on top of which the Spong Arc developed following Early Cretaceous subduction initiation.

Lower Cretaceous (mid-Valanginian–mid-Aptian range) radiolarian faunal assemblages reported by Baxter et al. (2010) provide robust biostratigraphic ages for the ophiolite-arc complex. This Lower Cretaceous assignment correlates with the younger population of K-Ar dates obtained by Reuber (1989) and our U-Pb zircon crystallization age. The similarity between ages for the early Spong Arc igneous rocks and cherts suggests that the cherts are a part of the lower section of the Spong Arc stratigraphy rather than being derived from older Jurassic ophiolite basement or older accreted fragments of the Neotethyan ocean crust scraped off the descending slab beneath the Spong Arc.

Gabbro from the Nidar ophiolite to the east has been dated at 130-110 Ma by the amphibole ^{40}Ar-^{39}Ar method (Mahéo et al., 2004) and 140 ± 32 Ma using a nine point mineral–whole rock Sm–Nd isochron with an initial $^{143}Nd/^{144}Nd$ of 0.513835±0.000053 (E_{Nd} t=+7.4) (Ahmad et al., 2008). Cherts within the overlying volcano-sedimentary unit yield Lower Cretaceous (132-127 Ma) radiolarians (Kojima et al., 2001) consistent with Spongtang cherts. This ophiolite structurally overlies the Tso Morari metamorphic complex to the south,

which contains subducted portions of the Indian continent including ~55 Ma coesite-bearing ultra-high pressure eclogites (de Sigoyer et al., 2000; Donaldson et al., 2013; Leech et al., 2007; St-Onge et al., 2013). de Sigoyer et al. (2004) interpret these eclogites to represent subducted portions of Indian crust beneath Eurasia and therefore the age of continent-continent collision (Leech et al., 2005). However, like Spongtang, the Nidar ophiolite is intra-oceanic in origin (Ahmad et al., 2008; Zyabrev et al., 2008). It is thrust over eclogite-bearing Indian crustal rocks at Tso Morari, indicating it was the first element to collide with India and this event may predate the final continental collision. It is becoming increasingly evident that ophiolites along the Indus-Yarlung-Tsangpo Suture represent an intra-oceanic supra-subduction zone ophiolite/island arc complex that was obducted onto the Indian margin as part of a north-dipping subduction zone that was distinct and separate from the Ladakh-Kohistan Arc that was also active but nearer the southern Eurasian margin (Aitchison et al., 2007a). A second, continental "Andean-type" convergent margin on the southern margin of Eurasia is supported by detrital zircon studies which indicate the Trans-Himalayan Arc was active until at least ~41 Ma in the Ladakh Batholith (Henderson et al., 2011) and ~37 Ma in the Gandese Batholith (Aitchison et al., 2011), well after collision of the ophiolite-arc complexes with India at ~55 Ma. The existence of two north-dipping subduction zones and two separate collisions is supported by the geological evidence. Nowhere along the entire Indus-Yarlung-Tsangpo suture do any of the Trans-Himalayan Arc igneous rocks intrude into the ophiolite-arc complexes as one would expect if they were the basement to a single subduction zone. The contact between the Ladakh Arc and ophiolitic complexes is always

faulted and this relationship is the same in Tibet. Indeed, the double subduction zone model is testable and falsifiable by the presence of an intrusive relationship between the Ladakh Arc and ophiolite complexes. This relationship would disprove the double subduction-collision model but it hasn't been recorded anywhere along the entire suture.

5.2 Intra-oceanic geodynamic setting of the Spong Arc

The transfer of juvenile, intra-oceanic ophiolitic and island-arc crust onto continental margins is an important mechanism for continental growth and the ages of ophiolites and the timing of emplacement onto continental margins are critical to accurate tectonic reconstructions of collision zones. This process is recorded in modern arc-continent collision systems, for example, Oman (Searle and Cox, 1999), New Caledonia (Aitchison et al., 1995), Taiwan (Huang et al., 2000) and Papua New Guinea (Holm et al., 2015) and is the key mechanism for the on-land preservation of dense, oceanic crust that would otherwise be recycled at subduction zones back into the mantle. Arc-continent collisions are responsible for widespread deformation events within ancient accretionary orogens such as eastern Australia (Aitchison and Buckman, 2012) and Central Asia (Buckman and Aitchison, 2004). Notably, these can be very short-lived events as documented by Dewey (2005). Lawsonite-bearing blueschists within the Shergol melange indicate cold subduction took place in an intra-oceanic setting beneath the Dras Arc (Groppo et al., 2016) at about 100 Ma (Honegger et al., 1989) and continued until the collision and partial subduction of the northern Indian continental margin to form the Tso Morari eclogites at ~55 Ma (de Sigoyer et al., 2000).

Further west in Pakistan, Kakar et al. (2012) extracted zircons from the Muslim Bagh ophiolite which yielded U-Pb crystallisation ages of ~80 Ma while geological relations constrain the emplacement age to between 68-48 Ma. They correlate the Muslim Bagh ophiolite with the Spong Arc as an intra-oceanic ophiolite-arc complex that first collided with India before the final India-Eurasia continental collision.

The isotopically juvenile nature of the ~136 Ma Spong Arc gabbros suggests that they developed far from the influence of any continental derived material and therefore, are unlikely to represent the fore-arc portion of the Trans-Himalayan Arc which grew at the southern Eurasian margin and shows clear isotopic evidence of continental influence within the Gangdese and Ladakh batholiths (Najman et al., 2017). This fits with existing paleomagnetic results indicating that the Ladakh Arc and southern margin of the Lhasa terrane were situated between 15-25°N throughout the Cretaceous, whereas the Indus-Yarlung-Tsangpo Suture ophiolites (Dazhuqu terrane) formed at equatorial settings some 1000-2500 km further south (Abrajevitch et al., 2005). Thus, the two subduction systems were unrelated.

5.3 Spong and Dras island arcs

The flat-lying Spongtang Massif is situated only 19 km south of the Dras-Nindam unit (Figure 10), being separated by a pop-up structure consisting of the Zanskar Supergroup that was thrust up and through the Dras-Nindam unit after final continental collision. The close proximity, similar ages and compositions of these rocks suggest that the Spong Arc may be equivalent to the Dras Arc (Figure 10) and this is consistent with the early cross-section

interpretations of Fuchs (1982) who previously classified the Spong Arc volcaniclastic rocks as “Dras Arc”. The intra-oceanic island arc affinities of both units hints at their being part of the same subduction system rather than belonging to a separate systems as was suggested by Corfield (2001).

The Spongtang Massif is unlikely to be part of the fore-arc region of the Kohistan-Ladakh-Gangdese Arc on the southern Eurasian margin (Fuchs, 1982; Steck, 2003) as it is more evolved and has a stronger continental influence as evident by the lower initial ε_{Hf} values (Bouilhol et al., 2011, 2013; Najman et al., 2017). Many tectonic models for the Indus Suture are heavily influenced by early interpretations that correlate the Kohistan, Ladakh and Dras arc systems as part of the same entity that evolved on the southern margin of Eurasia (Coward et al., 1987; Honegger et al., 1982; Khan et al., 1993; Searle et al., 1999). Granites of the Kohistan and Ladakh batholiths are of the same composition and age range as the Gandese Batholith in Tibet and therefore, are most likely to be part of the same Trans-Himalayan continental margin magmatic belt (Honegger et al., 1982; White et al., 2011). However, inconsistencies arise when forcing correlations with the Dras Arc and interpretations that it formed either the fore-arc basement of the Kohistan-Ladakh Arc or was an island arc that collided with Eurasia before evolving into the Kohistan-Ladakh- Arc (Fuchs, 1982; Honegger et al., 1982; Najman et al., 2017; Robertson and Degnan, 1994). This interpretation is based on the observation that the Dras volcanics are intruded by the ~103 Ma Kargil intrusive rocks (gabbro-norites to granodiorites), which are interpreted by Honegger et al. (1982) as equivalents of the Kohistan-Ladakh Arc and therefore, the Dras Arc had to have

collided with Eurasia during the Late Cretaceous prior to intrusion of the Kargil granodiorites and final collision with India.

Corfield et al. (2001) suggested that the Spong and Dras island arcs developed above two separate island-arc subduction systems unrelated to the Ladakh Arc on the southern margin of Eurasia. They suggest that these island-arc terranes only came together during final continental collision. However, zircon studies by Singh et al. (2007), Ravikant et al. (2009) and White et al. (2011) found no evidence for a ~100 Ma magmatic phase within the Ladakh Arc that might match the Kargil intrusive rocks. Instead, extensive granite magmatism occurred within the Ladakh Arc between 66-46 Ma with minor 85-75 Ma inheritance. This is reflected in detrital zircon studies of Indus Group sedimentary rocks, which show a distinct magmatic peak at 40-60 Ma and a smaller peak at 80-90 Ma but very few older zircons (Henderson et al., 2011). We suggest that correlation of the ~103 Ma Kargil intrusive rocks with 66-46 Ma granites of the Ladakh Batholith is not justified and that the Kargil intrusive rocks may represent the plutonic core of the intra-oceanic Dras island arc, which is unrelated to the Ladakh Arc that developed off the southern margin of Eurasia. Without the inferred correlation between Kargil intrusive rocks and Ladakh Batholith, there is no reason to support the interpretation of the Dras Arc first colliding with Eurasia and no reason to separate the Dras and Spong arcs as different island-arcs. Instead, we suggest that the Spong and Dras arcs are part of the same island arc complex that first collided with India during the early Eocene.

5.4 Timing of ophiolite-arc collision with India and closure of the Neotethys

The timing of collision of the Spongtang Massif with India is highly disputed as outlined in discussions between Garzanti and Searle (Garzanti et al., 2005). Corfield et al. (2001) argue for a Late Cretaceous collision between Spongtang Massif and India while Reuber et al. (1992) and Garzanti et al. (2005) argue for a collision later in the Eocene. The presence of Lower Eocene units (Chulung la Formation and Kong Slate) of the Zanskar Supergroup (India) beneath the Spongtang Massif thrust sheet was used as evidence that the ophiolite was not emplaced onto the Indian margin until post-Early Eocene (Colchen et al., 1987; Fuchs, 1982; Reuber, 1986; Reuber et al., 1992; Reuber et al., 2015). Several tectonic reconstructions place northern India at about 10°N (Aitchison et al., 2007a; Dewey et al., 1989; Molnar and Tapponnier, 1975) and at least 1000 km south of Eurasia at 45 Ma when the Ladakh Arc on the southern margin of Eurasia was at 23°N (Klootwijk et al., 1979). However, Corfield et al., (2001) contend that ophiolite obduction occurred much earlier in the Late Cretaceous and that the thrusting of the ophiolite over restricted Eocene marine basins that developed prior to and adjacent to the obducted ophiolite is related to later continent-continent collision. Corfield et al. (2001) interpret the closure of the Neotethys as a three-stage collision process starting with the obduction of the intra-oceanic Spongtang Massif onto India at about the same time that the intra-oceanic Dras-Kohistan Arc collided with the Trans-Himalayan Batholith to the north. This was followed by closure of the remaining Neotethys along southern Asia and final continent-continent collision of India with Eurasia during the Late Cretaceous (~70 Ma). In their model, the Spongtang Massif does not

represent the fore-arc basement of the continental margin of Eurasia (Ladakh Batholith) and is a separate subduction system to the intra-oceanic Dras-Kohistan Arc to the north, which first collides with the Trans-Himalayan continental arc of southern Eurasia before final continental collision of India and Eurasia. The Late Cretaceous (~70 Ma) timing of obduction of the Spongtang Massif onto India is proposed largely to fit with the long-held consensus that the India-Asia continental collision began at 55 Ma (de Sigoyer et al., 2000; Hu et al., 2016) and therefore, Eocene marine sediments (<55 Ma) could not have initially been overthrust by the ophiolite because they post-date the collision age. This model was disputed by Garzanti et al. (2005) on the basis of a lack of evidence for late thrusting. Also, the report of possible Late Eocene cherts within the mélange of the Lamayaru Complex immediately below the ophiolite by Colchen et al. (1987) is difficult to reconcile with the development of a small, shallow marine basins evolving adjacent to an ophiolite that was obducted onto India during the Late Cretaceous. We prefer the simplest explanation that the lower Eocene cherts within the mélange at the base of the Spongtang Massif and the lower Eocene Kong slate and Chulung la Formation below the ophiolite thrust sheet indicate post-early Eocene ophiolite obduction onto the Indian margin.

5.5 Paleogeography and subduction initiation within Neotethys

There is mounting evidence that all of the ophiolites along the IYTS formed within the Neotethyan Ocean before being obducted onto the Indian margin prior to final continental collision (Aitchison et al., 2007a). Thus, the position of the Lhasa terrane relative to India, Eurasia and the active arcs including the Kohistan-Ladakh-Gangdese and the Karakorum

batholiths is important when interpreting where intra-oceanic terranes were situated before being accreted onto either India or Asia (Figure 10). Recent paleomagnetic data indicate that the Lhasa terrane originated as a rifted portion of northern Gondwana (India or Australia) and was situated at about 16.5° south throughout the Triassic (Zhou et al., 2016). It drifted northwards to 3.7° south of the equator at 180 Ma (Li et al., 2016) and docked with the southern margin of Eurasia at about 25°N during the Late Cretaceous as constrained by the youngest (Lower Cretaceous) cherts within the Bangong-Nujiang Suture (Baxter et al., 2009). At 45-49 Ma the Ladakh Arc in the western Neotethyan ocean was at 23°N (Klootwijk et al., 1979), which marks the position of the southern margin of Eurasia. In contrast, the northern margin of India was only at ~10°N around 50 Ma, - see Acton (1999) and discussions by Aitchison et al. (2007a), indicating about 1500 km of ocean separated the northern passive margin of India and the southern convergent margin of Eurasia. This is consistent with the collision and obduction of the intra-oceanic Spongtang Massif with India at about 55 Ma in a separate event prior to final continental collision with Eurasia.

We follow the suggestion of Aitchison et al. (2012) that subduction may have initiated along major NNE-SSW trending transform faults that developed as the Lhasa terrane rifted away from Gondwana from Triassic to Jurassic (Figure 10). The orientation of major transform faults in the Neotethys can be constrained by the relative movement (rifting) of Lhasa terrane from Gondwana starting in the Early Permian, that is, they must be parallel to relative plate movement and perpendicular to the rift, as shown in tectonic reconstructions by Stampfli and Borel (2002), Heine et al. (2004), (Zahirovic et al., 2012) and Gibbons et al.

(2015). The juxtaposition of old and new ocean crust at transform faults has the potential of initiating spontaneous subduction via the process of transform collapse (Stern, 2004). Similar rotations of subduction systems are documented in the Izu-Bonin-Marianas system (Hall, 2002) which originates down near Papua New Guinea then rotates more than 90 degrees to its present positon. The "subduction initiation rule" proposed by Whattam and Stern (2011) predicts that supra-subduction zone (fore-arc) ophiolites display a sequence of igneous rocks that transition from fertile mantle-derived decompressional melts to increasingly metasomatised depleted mantle melts of boninitic composition to typical calc-alkaline arc magmas. The transition from Jurassic N-MORB Spongtang ophiolite to the Early Cretaceous calc-alkaline Spong Arc displays characteristics similar to the "subduction initiation rule". Thus, the Spongtang Massif has the potential to answer key questions including, A) the time it takes to initiate subduction, B) how initial fore-arc magmatism transitions to arc-like magmatism, C) how long arc magmatism persists and D) how intra-oceanic terranes are emplaced and preserved onto continental margins. Initiation of the Spong arc appears to involve an abrupt pulse of mafic magmatism at ~136 Ma, which is about 10 m.y. older than most ophiolites along the Yarlung-Tsangpo suture in Tibet, suggesting that subduction may have initiated in the west and migrated eastward along the length of the transform fault. Supra-subduction zone volcanism occurred sporadically between 136 Ma and 88 Ma (Pedersen et al., 2001). However, in order to accommodate plate convergence, subduction and arc volcanism may have continued until final collision with India at ~55 Ma. The youngest detrital zircon population in Kong Slate and Chulung la Formation is ~53 Ma

(Najman et al., 2017) suggesting that the youngest sedimentary units on the Indian passive margin may have been receiving zircons from the active Spong Arc right up until final collision. This suggests that the Spong Arc was active for some 80 million years as an intra-oceanic island arc within the Neotethys before collision with India, which is consistent with the timescales of oceanic island arc development in the Izu-Bonin-Marianas system as outlined by Ishizuka et al. (2011).

The Semail Ophiolite in Oman shows a similar geochemical evolution from N-MORB to supra-subduction (fore-arc, boninitic) magmas but it did not evolve into a well-developed calc-alkaline island arc. This is probably due to the short period of time between formation at ~95 Ma and obduction onto the Arabian continental margin at 85 Ma (Searle et al., 2003). To the NW, along the Iraqi segment of the Zagros Suture Zone, ophiolites such as Hasanbag ophiolite complex have an almost identical age to the Semail ophiolite (92 Ma; Ali et al. (2012)), while intra-oceanic terranes such as Walash-Naopurdan island arc are as young as 24 Ma (Ali et al., 2013) indicating continental collision started less than 24 million years ago in this region. The Semail and other ophiolites along the Zagros Suture Zone cannot be direct correlatives of the IYTS ophiolites because they were initiated along different subduction zones at different times and they formed either side of the Owen Fracture Zone (Gaina et al., 2015), which separated the rapidly northward moving Indian Plate from the slow-moving Arabian plate (Figure 10). However, they do represent the last Neotethyan ophiolites to be obducted onto the leading edge of a passive continental margin in events before and separate to terminal continental collision. At Oman, terminal continental collision has yet to occur

with a small amount of ocean floor yet to subduct beneath the active continental Makran Arc along the southern margin of Iran. Oman is a good example of an intra-oceanic ophiolite-arc complex colliding and obducting onto a continental margin long before final continental collision and is analogous to the collision of the Spongtang Massif with India well before terminal continental collision.

6 Conclusions

1) Zircons extracted from gabbro and leucogabbro from the Spongtang Massif both yield U-Pb SHRIMP ages of ~136 and 133 Ma (Early Cretaceous). This is younger than previous 177 Ma zircon (TIMS) ages reported by Pedersen et al. (2001).
2) Petrology and geochronology of the gabbro and basalts indicates two distinct mafic magmas are present – 1) N-MORB type volcanic rocks and minor gabbros of ~177 Ma age, 2) island-arc basalts, dolerite dykes and gabbros intruded through and onto the N-MORB volcanic pile. The older Jurassic crust represents the original Neotethys MORB-like crust while the Early Cretaceous gabbros and basalts represent renewed spreading associated with subduction initiation giving rise to the Spong Arc.
3) The depleted mantle-like, highly positive initial ε_{Hf} values indicate a purely intra-oceanic setting remote from continental crustal influence. The original Neotethyan Spongtang ophiolitic substrate is ~177 Ma and our acquired ~136 Ma zircon ages of leucogabbro represent intra-oceanic subduction initiation responsible for

development of the Spong Arc before its emplacement onto the Indian passive margin as the Spongtang Massif.

4) The timing of collision is constrained by the age of the youngest Indian sedimentary units over which the ophiolite has been obducted. These are the Eocene Kong Slates and Chulung la Formation, which contain detrital zircons as young as 53 Ma (Najman et al., 2017) and are likely to be derived from the final pulses of igneous activity within the Spong Arc before arc-continent collision extinguished any further igneous activity on the leading edge of India.

ACKNOWLEDGMENTS

This project was partially supported by the GeoQuEST Research Centre and a small research grant of the University of Wollongong. We thank Jigmet Punchok for his assistance in the field. Shane Paxton (Australian National University) is thanked for mineral separation. Les Kinsley (Australian National University) is thanked for technical assistance with the zircon Lu-Hf analyses. We thank Paul Carr for undertaking the XRF analysis and Keira Webb for sample preparation.

Table captions

Table 1 – whole rock geochemistry

Table 2 - U-Pb SHRIMP data

Table 3 - Hf data

Figure captions

Figure 1 Regional tectonic setting of the Himalaya showing Tethyan ophiolite occurrences and their age of formation (blue). Basemap sourced from GeoMapApp software (Ryan et al., 2009).

Figure 2 Geology of Spongtang ophiolite, Ladakh Himalaya. Adapted from (Corfield and Searle, 2000; Reuber et al., 2015; Steck, 2003)

Figure 3 Field relations of the Spongtang ophiolite. A) View of the Spongtang ophiolite looking south-east from Sir Sir la pass showing the ophiolite klippe thrust over the Zanskar Supergroup (Indian passive margin) and approximate position of dated samples. B) View looking SE of the outcrop from which the leucogabbro sample SBST12 was collected within the mélange at the base of the klippe along the Photang Valley; C) View of the Photong Thrust sheet which consists of Permian limestone and ocean island basalts (OIB) which have been thrust between the overlying Spongtang Ophiolite and underlying Lamayaru Complex. Includes the outcrop of the mélange containing the dated leucogabbro SBST12; D) Outcrop picture of the homogenous gabbro SBST05; E) View of the pegmatitic gabbro dykes and veins intruding massive gabbro sheets and peridotite in the upper Photang Valley.

Figure 4 Petrography of gabbro samples. A) Sample SBST19 olivine-hornblende gabbro containing highly altered plagioclase. B) SBST05 leucogabbro sample from which zircons were extracted showing heavily altered plagioclase, hornblende and free quartz. C) SBST17 leucogabbro (plane polarized) containing kaersutite. D) SBST16 gabbro (plane polarized light) containing several thin lenses of felsic melt. E) SBST16 gabbro (plane polarized light) containing thin lenses of felsic melt. F) SBST16 gabbro (cross polars) showing plagioclase and quartz crystallised in the stringers of melt with actinolite needles growing from the surrounding hornblende into the melt patch. G) SBST20 pegmatitic gabbro containing resorbed plagioclase, hornblende, kaersutite H) SBST20 pegmatitic gabbro (cross polars) showing the cross-hatch twinning of microcline that has crystallised with quartz in the melt veins.

Figure 5 Geochemical classification of gabbro and volcanic samples from Spongtang and the Dras Arc using data collated from this study and from Corfield et al. (2001). A) Immobile element rock classification diagram (Winchester and Floyd, 1977). B) IUGS gabbro classification. C) The tholeiitic-calc-alkaline classification (Irvine and Baragar, 1971)

Figure 6 Geochemical discrimination plots of basalts and gabbros collected from Spongtang ophiolite in this study and compiled with results of Corfield et al. (2001) which include Dras arc volcanics. A) V/Ti/1000 diagram of Shervais (1982); B) Ti/Zr plot of Pearce and Cann (1973); C) Th/Yb / Nb/Yb MORB array plot of Pearce (2008); D) Zr-Th-Nb ternary discrimination diagram of (Wood, 1980); E) Chondrite normalized and F) NMORB normalised rare-earth plot of Sun and McDonough (1989).

Figure 7 Cathodoluminescence (CL) image of representative zircons from samples SBST05 and -12, with the analytical sites indicated. * indicates site where loss of radiogenic Pb is detected.

Figure 8 TW. $^{238}U/^{206}Pb$ – $^{207}Pb/^{206}Pb$ plot, uncorrected for common Pb. Analytical errors are depicted at the 2 sigma level.

Figure 9 Hf. ε_{Hf} – time plot for the SBST12 zircon data. 'Linear DM' (depleted mantle) is a chord between a modern ε_{Hf} = +17 and ε_{Hf} = 0 at 4560 Ma. CHUR is the Chondritic Uniform Reservoir reference. The field 'juvenile arc rocks' is bounded by linear DM and the evolution line of (Dhuime et al., 2011) for island arcs – a chord from modern ε_{Hf} = +13 and ε_{Hf} = 0 at 4560 Ma. A typical ±2σ error bar for the data is shown.

Figure 10 Time-space diagram showing all published ages for the Spongtang ophiolite and Dras-Nindam arc. K-Ar dates are from Reuber et al., 1989 and U/Pb dates from Pederson et al., 2001. Plate reconstructions are modified from the GPlates model of Seton et al. (2012). Modifications of the model are based on new paleomagnetic data for the Lhasa terrane (LT) by Zhou et al., 2016 and Li et al., 2015 who have the Lhasa terrane much further south from the Triassic to Cretaceous than in the model of Seton et al. (2012). Likewise paleomagnetic data from Klootwijk et al., 1979 has the Ladakh Arc positioned further south at 23°N. In this reconstruction the Spongtang ophiolite and Dras Arc evolve as an intra-oceanic island arc system that developed as a result of spontaneous subduction at ~136 Ma along a NNE-SSW transform fault in the Neotethys Ocean. This ophiolite-arc complex collided with India at ~55 Ma at roughly equatorial latitude while the Ladakh Arc (Trans-Himalayan Arc) developed closer to the southern margin of Eurasia before final collision at ~35 Ma.

7 Appendices

7.1 XRF Analytical Methods

Nine basalt and eight gabbro samples were collected from the Spongtang ophiolite within the Photang Valley. Samples were crushed using a TEMA chromium ring mill. Fused buttons were made for X-ray fluorescence (XRF) major element analysis. Depending on elemental concentrations estimated in trace element analysis, different types of flux were used. Pure metaborate was used for high silica samples, 57% tetraborate to 43% metaborate was used for ultramafic samples, and 12% tetraborate to 22% metaborate was used for mafic samples. 400mg of sample was added to each flux (300 mg for puremetaborate). Samples JP22, JP35 and JP44were oxidised before being fused in the furnace by adding 5 ml of lithium nitrate solution and left at 60 °C overnight. Pressed pellets for trace element analysis were created by mixing ~5 g of sample with a polyvinyl acetate (PVA) binder and pressed into an aluminium cup using a hydraulic hand press. Trace element pressed pellets were then oven dried at 60 °C for 12 hours. Whole rock geochemical analysis was conducted using a SPECTRO XEPOS energy dispersive polarisation X-ray fluorescence spectrometer at the University of Wollongong. Additional trace elements and the rare-earth element analyses were undertaken at Australian Laboratory Services (ALS) at Brisbane, Australia using inductively coupled plasma–mass spectroscopy (ICP-MS).

7.2 SHRIMP U-Pb analytical method and data appraisal

Heavy minerals were concentrated using heavy liquid and isodynamic separation techniques at the mineral separation laboratory of the Research School of Earth Sciences, the Australian National University (ANU). Using a binocular microscope, the concentrates were hand-picked, and the chosen grains were cast into an epoxy resin disc along with reference Temora zircons (Black et al., 2003). After the epoxy cured, the mount was ground to a mid-section level through the grains and then polished. Cathodoluminescence (CL) imaging was used to document the grains.

U-Th-Pb analyses of the zircons were undertaken on the Hiroshima University SHRIMP 2 instrument (now moved to Nagoya University) following analytical protocols of Williams (1998), with the raw data being reduced using ANU software 'PRAWN' and 'Lead'. Measurements of $^{206}Pb/^{238}U$ in unknown zircons were calibrated using the Temora standard (U-Pb ages concordant at 417 Ma; (Black et al., 2003)). The reference zircon SL13 (U=238 ppm) located in a set-up mount was used to calibrate U and Th abundance in the unknown zircons. The ISOPLOT program (Ludwig, 2003) was used to assess and plot the reduced and calibrated data. The results are plotted in a Tera-Wasserburg Concordia diagram prior to correction for common Pb. The reason for plotting them without correction for common Pb is to demonstrate that given the small amount of common Pb in these zircons, the data already have close to concordant U-Pb ages, prior to correction. Weighted mean $^{206}Pb/^{238}U$ ages were calculated following the '207' method of Compston et al. (1984) and using the Cumming and Richards (1975) Pb composition for the likely age of the zircons.

7.3 LA-MC-ICP-MS zircon Lu-Hf isotopes

Zircon hafnium isotopic compositions were determined over a single analytical session 5-6 May 2016, using the RSES ThermoFinnigan Neptune multi-collector ICPMS coupled to a Lambda Physik ArF, 193 nm excimer laser system with a 'HelEx' sample cell, following methods described by Hiess et al. (2009). Hf isotope analytical sites coincided with the U-Pb age determination sites where available. NIST 612 glass and a large zircon crystal from the Monastery kimberlite were used to initially tune the mass spectrometer to optimum sensitivity, adjust peak shape and ensure good collector positioning for all isotopes to be measured including those of Lu and Yb in addition to Hf. Analyses were made with a 47 μm diameter circular spot firing at 5 Hz with an energy density at the sample surface of ~10 J/cm2. For small zircons the spot overlapped onto the epoxy, but there was no detectable blank contribution. ^{171}Yb, ^{173}Yb, ^{174}Hf, ^{175}Lu, ^{176}Hf, ^{177}Hf, ^{178}Hf, ^{179}Hf and ^{181}Ta isotopes were simultaneously measured in static-collection mode on 9 Faraday cups with 10^{11} Ω resistors. Analysis of a gas blank and a suite of 6 secondary reference zircons with a range of ^{176}Hf/^{177}Hf, ^{176}Lu/^{177}Hf ratios ^{176}Yb/^{177}Hf (Monastery, Mud Tank, Plesovice, QGNG,, R33 and FC1) were performed systematically after every 10-12 sample spot analyses throughout the session.

Data were acquired in 1 s integrations over 60 s or until the grain burned through. Time slices were later cropped to periods maintaining steady ^{176}Hf/^{177}Hf signals during data reduction on a custom Excel™ spreadsheet. Total Hf signal intensity typically fell from >10 to ~6 volts during a single analysis. The measured ^{176}Lu/^{177}Hf, ^{176}Hf/^{177}Hf, ^{178}Hf/^{177}Hf and ^{174}Hf/^{177}Hf ratios for all standard and sample analyses are presented in Supplementary Table 3. Mass bias was corrected using an

exponential law (Chu et al., 2002; Russell et al., 1978; Woodhead et al., 2004) and a composition for $^{179}Hf/^{177}Hf$ of 0.732500 (Patchett et al., 1982). Yb and Lu mass bias factors were assumed to be identical and normalised using an exponential correction referenced to a $^{173}Yb/^{171}Yb$ ratio of 1.129197 (Vervoort et al., 2004). The intensity of the ^{176}Hf peak was determined accurately by removing isobaric interferences from ^{176}Lu and ^{176}Yb. Interference-free ^{175}Lu and ^{173}Yb were measured and the interference peaks subtracted according to reported $^{176}Lu/^{175}Lu$ and $^{176}Yb/^{173}Yb$ isotopic abundances of Vervoort et al. (2004). As a quality check of this procedure, $^{178}Hf/^{177}Hf$ and $^{174}Hf/^{177}Hf$ ratios for all zircon reference materials and samples were monitored. In particular the $^{174}Hf/^{177}Hf$ ratio is a sensitive monitor of the efficacy of Yb corrections owing to the relatively large ^{174}Yb isotopic interference (31.83% abundance) that must be removed from the small ^{174}Hf isotope (0.16% abundance). The mean $^{178}Hf/^{177}Hf$ and $^{174}Hf/^{177}Hf$ ratios for all standards and samples lie within uncertainty of the values published by Thirlwall and Anczkiewicz (2004) and Vervoort et al, (2004); Supplementary Table 3, regardless of zircon REE content demonstrating the accuracy of Yb corrections. Furthermore, no correlation exists between $^{176}Hf/^{177}Hf$ and $^{178}Hf/^{177}Hf$, $^{174}Hf/^{177}Hf$, $^{176}Lu/^{177}Hf$ ratios for any zircon reference materials, including higher Lu/Hf standards FC1 and R33. Based on results from the six reference zircons, which were all within error of accepted solution values reported by Woodhead et al. (2004), no additional external corrections to the measured $^{176}Hf/^{177}Hf$ were required.

Zircon $^{176}Lu/^{177}Hf$ ratios must be accurately determined by LA-MC-ICPMS, to enable corrections for in-growth of radiogenic ^{176}Hf. Average measured $^{176}Lu/^{177}Hf$ ratios within reference zircons with a range of reported compositions based on solution analyses are in good agreement with

the measured laser analyses The mean $^{176}Hf/^{177}Hf$ ratios for the six reference zircons deviate from published solution values by +0.0 (Plesovice); +0.30 (Mud Tank), +0.33 (QGNG), +0.15 (FC-1), -0.24 (TEM-2), -0.16 (R33) and -0.08 (Monastery) ε_{Hf} units (Supplementary Table 3).

The segmental processing of the laser ablation data means that any down-hole variation in Lu/Hf and $^{176}Hf/^{177}Hf$ ratio can be detected and tracked. In all sample spot analyses Lu/Hf and $^{176}Hf/^{177}Hf$ ratios were uniform throughout data acquisition.

REFERENCES CITED

Abrajevitch, A.V., Ali, J.R., Aitchison, J.C., Badengzhu, Davis, A.M., Liu, J.B., Ziabrev, S.V., 2005. Neotethys and the India-Asia collision: Insights from a palaeomagnetic study of the Dazhuqu ophiolite, southern Tibet. Earth Planet. Sci. Lett. 233, 87-102.

Acton, G.D., 1999. Apparent polar wander of India since the Cretaceous with implications for regional tectonics and true polar wander, In: Radhakrishna, T., Piper, J.D.A. (Eds.), The Indian Subcontinent and Gondwana: A Palaeomagnetic and Rock Magnetic Perspective. Geological Society of India, Bangalore, pp. 129-175.

Ahmad, T., Tanaka, T., Sachan, H.K., Asahara, Y., Islam, R., Khanna, P.P., 2008. Geochemical and isotopic constraints on the age and origin of the Nidar Ophiolitic Complex, Ladakh, India: Implications for the Neo-Tethyan subduction along the Indus suture zone. Tectonophysics 451, 206-224.

Aitchison, J., Gibbons, A., Müller, R., Whittaker, J., 2012. Birth of a Neotethyan intra-oceanic arc, AGU Fall Meeting Abstracts.

Aitchison, J.C., Ali, J.R., Davis, A.M., 2007a. When and where did India and Asia collide? Journal of Geophysical Research 112.

Aitchison, J.C., Badengzhu, Davis, A.M., Liu, J.B., Luo, H., Malpas, J.G., McDermid, I.R.C., Wu, H.Y., Ziabrev, S.V., Zhou, M.F., 2000. Remnants of a Cretaceous intra-oceanic subduction system within the Yarlung-Zangbo suture (southern Tibet). Earth Planet. Sci. Lett. 183, 231-244.

Aitchison, J.C., Buckman, S., 2012. Accordion vs. quantum tectonics: Insights into continental growth processes from the Paleozoic of eastern Gondwana. Gondwana Research 22, 674-680.

Aitchison, J.C., Clarke, G.L., Meffre, S., Cluzel, D., 1995. Eocene Arc-Continent Collision in New-Caledonia and Implications for Regional Southwest Pacific Tectonic Evolution. Geology 23, 161-164.
Aitchison, J.C., Davis, A.M., Abrajevitch, A.V., Ali, J.R., Badengzhu, Liu, J., Luo, H., McDermid, I.R.C., Zyabrev, S.V., 2003. Stratigraphic and sedimentological constraints on the age and tectonic evolution of the Neotethyan ophiolites along the Yarlung Tsangpo suture zone, Tibet, In: Dilek, Y., Robinson, P.T. (Eds.), Ophiolites in Earth History, pp. 147-164.
Aitchison, J.C., Davis, A.M., Badengzhu, B., Luo, H., 2002. New constraints on the India-Asia collision: the Lower Miocene Gangrinboche conglomerates, Yarlung Tsangpo suture zone, SE Tibet. J. Asian Earth Sci. 21, 251-263.
Aitchison, J.C., McDermid, I.R.C., Ali, J.R., Davis, A.M., Zyabrev, S.V., 2007b. Shoshonites in Southern Tibet Record Late Jurassic Rifting of a Tethyan Intraoceanic Island Arc. The Journal of Geology 115, 197-213.
Aitchison, J.C., Xia, X.P., Baxter, A.T., Ali, J.R., 2011. Detrital zircon U-Pb ages along the Yarlung-Tsangpo suture zone, Tibet: Implications for oblique convergence and collision between India and Asia. Gondwana Research 20, 691-709.
Ali, S.A., Buckman, S., Aswad, K.J., Jones, B.G., Ismail, S.A., Nutman, A.P., 2012. Recognition of Late Cretaceous Hasanbag ophiolite-arc rocks in the Kurdistan Region of the Iraqi Zagros suture zone: A missing link in the paleogeography of the closing Neotethys Ocean. Lithosphere 4, 395-410.
Ali, S.A., Buckman, S., Aswad, K.J., Jones, B.G., Ismail, S.A., Nutman, A.P., 2013. The tectonic evolution of a Neo-Tethyan (Eocene-Oligocene) island-arc (Walash and Naopurdan groups) in the Kurdistan region of the Northeast Iraqi Zagros Suture Zone. Isl. Arc. 22, 104-125.
Ballard, J.R., Palin, J.M., Campbell, I.H., 2002. Relative oxidation states of magmas inferred from Ce(IV)/Ce(III) in zircon: application to porphyry copper deposits of northern Chile. Contrib Mineral Petr 144, 347-364.
Bassoullet, J.P., Colchen, M., Juteau, T., Marcoux, J., Mascle, G., 1980. Structure of the Zanskar Nappes, Ladakh, Himalaya. Comptes Rendus Hebdomadaires Des Seances De L Academie Des Sciences Serie D 290, 389-392.
Baud, A., Arn, R., Bugnon, P., Crisinel, A., Dolivo, E., Escher, A., Hammerschlag, J., Marthaler, M., Masson, H., Steck, A., 1982. Le contact Gondwana-péri-Gondwana dans le Zanskar oriental (Ladakh, Himalaya). B Soc Geol Fr 24, 341-361.
Baxter, A.T., Aitchison, J.C., Ali, J.R., Chan, J.S.L., Chan, G.H.N., 2016. Detrital chrome spinel evidence for a Neotethyan intra-oceanic island arc collision with India in the Paleocene. J. Asian Earth Sci. 128, 90-104.
Baxter, A.T., Aitchison, J.C., Ali, J.R., Zyabrev, S.V., 2010. Early Cretaceous radiolarians from the Spongtang massif, Ladakh, NW India: implications for Neo-Tethyan evolution. J Geol Soc London 167, 511-517.

Baxter, A.T., Aitchison, J.C., Zyabrev, S.V., 2009. Radiolarian age constraints on Mesotethyan ocean evolution, and their implications for development of the Bangong-Nujiang suture, Tibet. J Geol Soc London 166, 689-694.
Bédard, É., Hébert, R., Guilmette, C., Lesage, G., Wang, C.S., Dostal, J., 2009. Petrology and geochemistry of the Saga and Sangsang ophiolitic massifs, Yarlung Zangbo Suture Zone, Southern Tibet: Evidence for an arc–back-arc origin. Lithos 113, 48-67.
Black, L.P., Kamo, S.L., Allen, C.M., Aleinikoff, J.N., Davis, D.W., Korsch, R.J., Foudoulis, C., 2003. TEMORA 1: a new zircon standard for Phanerozoic U-Pb geochronology. Chem. Geol. 200, 155-170.
Borneman, N.L., Hodges, K.V., van Soest, M.C., Bohon, W., Wartho, J.-A., Cronk, S.S., Ahmad, T., 2015. Age and structure of the shyok suture in the ladakh region of northwestern India: Implications for slip on the karakoram fault system. Tectonics, n/a-n/a.
Bouilhol, P., Jagoutz, O., Hanchar, J.M., Dudas, F.O., 2013. Dating the India-Eurasia collision through arc magmatic records. Earth Planet. Sci. Lett. 366, 163-175.
Bouilhol, P., Schaltegger, U., Chiaradia, M., Ovtcharova, M., Stracke, A., Burg, J.P., Dawood, H., 2011. Timing of juvenile arc crust formation and evolution in the Sapat Complex (Kohistan-Pakistan). Chem. Geol. 280, 243-256.
Bouvier, A., Vervoort, J.D., Patchett, P.J., 2008. The Lu-Hf and Sm-Nd isotopic composition of CHUR: Constraints from unequilibrated chondrites and implications for the bulk composition of terrestrial planets. Earth Planet. Sci. Lett. 273, 48-57.
Brookfield, M.E., Andrews-Speed, C.P., 1984. Sedimentology, Petrography and Tectonic Significance of the Shelf, Flysch and Molasse Clastic Deposits across the Indus Suture Zone, Ladakh, Nw India. Sedimentary Geology 40, 249-286.
Chu, N.C., Taylor, R.N., Chavagnac, V., Nesbitt, R.W., Boella, R.M., Milton, J.A., German, C.R., Bayon, G., Burton, K., 2002. Hf isotope ratio analysis using multi-collector inductively coupled plasma mass spectrometry: an evaluation of isobaric interference corrections. Journal of Analytical Atomic Spectrometry 17, 1567-1574.
Clift, P., Hannigan, R., Blusztajn, J., Draut, A.E., 2002a. Geochemical evolution of the Dras-Kohistan Arc during collision with Eurasia: Evidence from the Ladakh Himalaya, India. The Island Arc 11, 255-273.
Clift, P.D., Carter, A., Krol, M., Kirby, E., 2002b. Constraints on India-Eurasia collision in the Arabian Sea region taken from the Indus Group, Ladakh Himalaya, India. Tectonic and Climatic Evolution of the Arabian Sea Region 195, 97-116.
Clift, P.D., Degnan, P.J., Hannigan, R., Blusztajn, J., 2000. Sedimentary and geochemical evolution of the Dras forearc basin, Indus suture, Ladakh Himalaya, India. Geol. Soc. Am. Bull. 112, 450-466.
Clift, P.D., Shimizu, N., Layne, G.D., Blusztajn, J., 2001. Tracing patterns of erosion and drainage in the Paleogene Himalaya through ion probe Pb isotope analysis of detrital K-feldspars in the Indus Molasse, India. Earth Planet. Sci. Lett. 188, 475-491.

Colchen, M., Reuber, I., Bassoullet, J.P., Bellier, J.-P., Blondeau, A., Lys, M., De Wever, P., 1987. Donnees biostratigraphiques sur les melanges ophiolitiques du Zanskar, Himalaya du Ladakh.
(Biostratigraphic data on the Zanskar ophiolitic melanges, Ladakh- Himalaya (India)). Comptes Rendus - Academie des Sciences, Serie II 305, 403-406.
Compston, W., Williams, I., Meyer, C., 1984. U-Pb geochronology of zircons from lunar breccia 73217 using a sensitive high mass-resolution ion microprobe. Journal of Geophysical Research: Solid Earth 89.
Corfield, R.I., Searle, M.P., 2000. Crustal shortening estimates across the north Indian continental margin, Ladakh, NW India. Tectonics of the Nanga Parbat Syntaxis and the Western Himalaya 170, 395-410.
Corfield, R.I., Searle, M.P., Green, O.R., 1999. Photang thrust sheet: an accretionary complex structurally below the Spontang ophiolite constraining timing and tectonic environment of ophiolite obduction, Ladakh Himalaya, NW India. J Geol Soc London 156, 1031-1044.
Corfield, R.I., Searle, M.P., Pedersen, R.B., 2001. Tectonic setting, origin, and obduction history of the spontang ophiolite, Ladakh Himalaya, NW India. Journal of Geology 109, 715-736.
Coward, M.P., Butler, R.W.H., Khan, M.A., Knipe, R.J., 1987. The Tectonic History of Kohistan and Its Implications for Himalayan Structure. J Geol Soc London 144, 377-391.
Cumming, G.L., Richards, J.R., 1975. Ore Lead Isotope Ratios in a Continuously Changing Earth. Earth Planet. Sci. Lett. 28, 155-171.
Davis, A.M., Aitchison, J.C., Hui, L., 2004. Conglomerates record the tectonic evolution of the Yarlung-Tsangpo suture zone in southern Tibet. Geol Soc Spec Publ 226, 235-246.
de Sigoyer, J., Chavagnac, V., Blichert-Toft, J., Villa, I.M., Luais, B., Guillot, S., Cosca, M., Mascle, G., 2000. Dating the Indian continental subduction and collisional thickening in the northwest Himalaya: Multichronology of the Tso Morari eclogites. Geology 28, 487.
de Sigoyer, J., Guillot, S., Dick, P., 2004. Exhumation of the ultrahigh-pressure Tso Morari unit in eastern Ladakh (NW Himalaya): A case study. Tectonics 23, n/a-n/a.
Dewey, J.F., 2005. Orogeny can be very short. Proc Natl Acad Sci U S A 102, 15286-15293.
Dewey, J.F., Cande, S., Pitman, W.C., 1989. Tectonic Evolution of the India Eurasia Collision Zone. Eclogae Geol. Helv. 82, 717-734.
Dhuime, B., Hawkesworth, C., Cawood, P., 2011. Geochemistry. When continents formed. Science 331, 154-155.
Dilek, Y., Furnes, H., 2011. Ophiolite genesis and global tectonics: Geochemical and tectonic fingerprinting of ancient oceanic lithosphere. Geol. Soc. Am. Bull. 123, 387-411.
Donaldson, D.G., Webb, A.A.G., Menold, C.A., Kylander-Clark, A.R.C., Hacker, B.R., 2013. Petrochronology of Himalayan ultrahigh-pressure eclogite. Geology 41, 835-838.
Dubois-Cote, V., Hebert, R., Dupuis, C., Wang, C.S., Li, Y.L., Dostal, J., 2005. Petrological and geochemical evidence for the origin of the Yarlung Zangbo ophiolites, southern Tibet. Chem. Geol. 214, 265-286.

Dunlap, W.J., Wysoczanski, R., 2002. Thermal evidence for early Cretaceous metamorphism in the Shyok suture zone and age of the Khardung volcanic rocks, Ladakh, India. J. Asian Earth Sci. 20, 481-490.
Dupuis, C., Hebert, R., Dubois-Cote, V., Guilmette, C., Wang, C.S., Li, Y.L., Li, Z.J., 2005. The Yarlung Zangbo Suture Zone ophiolitic melange (southern Tibet): new insights from geochemistry of ultramafic rocks. J. Asian Earth Sci. 25, 937-960.
Dürr, S.B., 1996. Provenance of Xigaze fore-arc basin clastic rocks (Cretaceous, South Tibet). Geol. Soc. Am. Bull. 108, 669-684.
Ehiro, M., Kojima, S., Sato, T., Ahmad, T., Ohtani, T., 2007. Discovery of Jurassic ammonoids from the Shyok suture zone to the northeast of Chang La Pass, Ladakh, northwest India and its tectonic significance. Isl. Arc. 16, 124-132.
Einsele, G., Liu B, Dürr, S., Frisch, W., Liu G, Luterbacher, H.P., Ratschbacher, L., Ricken, W., Wendt, J., Wetzel, A., Yu, G., Zheng, H., 1994. The Xigaze forearc basin: evolution and facies architecture (Cretaceous, Tibet). Sedimentary Geology 90, 1-32.
Fuchs, G., 1979. On the Geology of Western Ladakh. Jahrbuch der Geologischen Bundesanstalt A 122, 513-540.
Fuchs, G., 1981. Outline of the Geology of the Himalaya. Mitt. Österr. Geol. Ges. 74/75, 101-127.
Fuchs, G., 1982. The Geology of Western Zanskar. The Geology of Western Zanskar 125, 1-50.
Fuchs, G., 1986. Geology of the Markha-Khurnak Region in Ladakh (India). Jahrbuch der Geologischen Bundesanstalt A 128, 403-437.
Fuchs, G., Willems, H., 1990. The Final Stages of Sedimentation in the Tethyan Zone of Zanskar and their Geodynamic Significance (Ladakh-Himalaya). Jahrbuch der Geologischen Bundesanstalt 133, 259-273.
Gaetani, M., Garzanti, E., 1991. Multicyclic History of the Northern India Continental-Margin (Northwestern Himalaya). Aapg Bulletin-American Association of Petroleum Geologists 75, 1427-1446.
Gaina, C., van Hinsbergen, D.J.J., Spakman, W., 2015. Tectonic interactions between India and Arabia since the Jurassic reconstructed from marine geophysics, ophiolite geology, and seismic tomography. Tectonics 34, 875-906.
Gansser, A., 1964. The Geology of the Himalayas. Wiley-Interscience, New York. 289 pp.
Garzanti, E., Baud, A., Mascle, G., 1987. Sedimentary Record of the Northward Flight of India and Its Collision with Eurasia (Ladakh Himalaya, India). Geodin Acta 1, 297-312.
Garzanti, E., Sciunnach, D., Gaetani, M., Corfield, R.I., Watts, A.B., Searle, M.P., 2005. Discussion on subsidence history of the north Indian continental margin, Zanskar-Ladakh Himalaya, NW India. J Geol Soc London 162, 889-892.
Garzanti, E., Van Haver, T., 1988. The indus clastics: forearc basin sedimentation in the Ladakh Himalaya (India). Sedimentary Geology 59, 237-249.

Gibbons, A.D., Zahirovic, S., Muller, R.D., Whittaker, J.M., Yatheesh, V., 2015. A tectonic model reconciling evidence for the collisions between India, Eurasia and intra-oceanic arcs of the central-eastern Tethys. Gondwana Research 28, 451-492.
Girardeau, J., Marcoux, J., Yougong, Z., 1984. Lithologic and Tectonic Environment of the Xigaze Ophiolite (Yarlung Zangbo Suture Zone, Southern Tibet, China), and Kinematics of Its Emplacement. Eclogae Geol. Helv. 77, 153-170.
Girardeau, J., Mercier, J.C.C., Yougong, Z., 1985a. Origin of the Xigaze Ophiolite, Yarlung Zangbo Suture Zone, Southern Tibet. Tectonophysics 119, 407-433.
Girardeau, J., Mercier, J.C.C., Zao, Y.O., 1985b. Structure of the Xigaze Ophiolite, Yarlung Zangbo Suture Zone, Southern Tibet, China - Genetic-Implications. Tectonics 4, 267-&.
Groppo, C., Rolfo, F., Sachan, H.K., Rai, S.K., 2016. Petrology of blueschist from the Western Himalaya (Ladakh, NW India): exploring the complex behavior of a lawsonite-bearing system in a paleo-accretionary setting. Lithos 252, 41-56.
Hall, R., 2002. Cenozoic geological and plate tectonic evolution of SE Asia and the SW Pacific: computer-based reconstructions, model and animations. J. Asian Earth Sci. 20, 353-431.
Hébert, R., Bezard, R., Guilmette, C., Dostal, J., Wang, C.S., Liu, Z.F., 2012. The Indus–Yarlung Zangbo ophiolites from Nanga Parbat to Namche Barwa syntaxes, southern Tibet: First synthesis of petrology, geochemistry, and geochronology with incidences on geodynamic reconstructions of Neo-Tethys. Gondwana Research 22, 377-397.
Heine, C., Muller, R.D., Gaina, C., 2004. Reconstructing the Lost Eastern Tethys Ocean Basin: Convergence history of the SE Asian margin and marine gateways. Geoph Monog Series 149, 37-54.
Heitz, A., 1986. Datations par méthode K/Ar sur filons du massif ophiolitique de Spongtang, rapport Strasbourg, p. 28.
Henderson, A.L., Najman, Y., Parrish, R., BouDagher-Fadel, M., Barford, D., Garzanti, E., Ando, S., 2010. Geology of the Cenozoic Indus Basin sedimentary rocks: Paleoenvironmental interpretation of sedimentation from the western Himalaya during the early phases of India-Eurasia collision. Tectonics 29.
Henderson, A.L., Najman, Y., Parrish, R., Mark, D.F., Foster, G.L., 2011. Constraints to the timing of India-Eurasia collision; a re-evaluation of evidence from the Indus Basin sedimentary rocks of the Indus-Tsangpo Suture Zone, Ladakh, India. Earth-Science Reviews 106, 265-292.
Heri, A.R., Aitchison, J.C., King, J.A., Villa, I.M., 2015. Geochronology and isotope geochemistry of Eocene dykes intruding the Ladakh Batholith. Lithos 212-215, 111-121.
Hiess, J., Bennett, V.C., Nutman, A.P., Williams, I.S., 2009. In situ U-Pb, O and Hf isotopic compositions of zircon and olivine from Eoarchaean rocks, West Greenland: New insights to making old crust. Geochim Cosmochim Ac 73, 4489-4516.
Hole, M.J., Saunders, A.D., Marriner, G.F., Tarney, J., 1984. Subduction of pelagic sediments: Implications for the origins of Ce-anomolous basalts from the Marianas islands. Journal of the Geological Society, London 141, 453-472.

Holm, R.J., Spandler, C., Richards, S.W., 2015. Continental collision, orogenesis and arc magmatism of the Miocene Maramuni arc, Papua New Guinea. Gondwana Research 28, 1117-1136.
Honegger, K., Dietrich, V., Frank, W., Gansser, A., Thoni, M., Trommsdorff, V., 1982. Magmatism and Metamorphism in the Ladakh Himalayas (the Indus-Tsangpo Suture Zone). Earth Planet. Sci. Lett. 60, 253-292.
Honegger, K., Le Fort, P., Mascle, G., Zimmermann, J.L., 1989. The blueschists along the Indus suture zone in Ladakh, NW Himalaya. Journal of Metamorphic Geology 7, 57-73.
Hu, X.M., Garzanti, E., Wang, J.G., Huang, W.T., An, W., Webb, A., 2016. The timing of India-Asia collision onset - Facts, theories, controversies. Earth-Science Reviews 160, 264-299.
Huang, C.Y., Yuan, P.B., Lin, C.W., Wang, T.K., Chang, C.P., 2000. Geodynamic processes of Taiwan arc-continent collision and comparison with analogs in Timor, Papua New Guinea, Urals and Corsica. Tectonophysics 325, 1-21.
Iizuka, T., Komiya, T., Rino, S., Maruyama, S., Hirata, T., 2010. Detrital zircon evidence for Hf isotopic evolution of granitoid crust and continental growth. Geochim Cosmochim Ac 74, 2450-2472.
Irvine, T.N., Baragar, W.R.A., 1971. A Guide to the Chemical Classification of the Common Volcanic Rocks. Can J Earth Sci 8, 523-548.
Ishizuka, O., Hickey-Vargas, R., Arculus, R.J., Yogodzinski, G.M., Savov, I.P., Kusano, Y., McCarthy, A., Brandl, P.A., Sudo, M., 2018. Age of Izu–Bonin–Mariana arc basement. Earth Planet. Sci. Lett. 481, 80-90.
Ishizuka, O., Tani, K., Reagan, M.K., Kanayama, K., Umino, S., Harigane, Y., Sakamoto, I., Miyajima, Y., Yuasa, M., Dunkley, D.J., 2011. The timescales of subduction initiation and subsequent evolution of an oceanic island arc. Earth Planet. Sci. Lett. 306, 229-240.
Jan, M.Q., Windley, B.F., Khan, A., 1985. The Waziristan Ophiolite, Pakistan - General Geology and Chemistry of Chromite and Associated Phases. Econ Geol 80, 294-306.
Ji, W.Q., Wu, F.Y., Chung, S.L., Li, J.X., Liu, C.Z., 2009. Zircon U-Pb geochronology and Hf isotopic constraints on petrogenesis of the Gangdese batholith, southern Tibet. Chem. Geol. 262, 229-245.
Jones, R.E., Kirstein, L.A., Kasemann, S.A., Dhuime, B., Elliott, T., Litvak, V.D., Alonso, R., Hinton, R., Facility, E.I.M., 2015. Geodynamic controls on the contamination of Cenozoic arc magmas in the southern Central Andes: Insights from the O and Hf isotopic composition of zircon. Geochim Cosmochim Ac 164, 386-402.
Kakar, M.I., Collins, A.S., Mahmood, K., Foden, J.D., Khan, M., 2012. U-Pb zircon crystallization age of the Muslim Bagh ophiolite: Enigmatic remains of an extensive pre-Himalayan arc. Geology 40, 1099-1102.
Kelemen, P.B., Sonnenfeld, M.D., 1983. Stratigraphy, structure, petrology and local tectonics, central Ladakh, NW Himalaya. Schweiz. Mineral. Petrog. Mitt. 63, 267-287.
Khan, M.A., Jan, M.Q., Weaver, B.L., 1993. Evolution of the lower arc crust in Kohistan, N. Pakistan; temporal arc magmatism through early, mature and intra-arc rift stages, In: Treloar,

P.J., Searle, M.P. (Eds.), Himalayan tectonics. Geological Society of London, London, United Kingdom, pp. 123-138.
Klootwijk, C., Sharma, M.L., Gergan, J., Tirkey, B., Shah, S.K., Agarwal, V., 1979. The extent of Greater India, II. Palaeomagnetic data from the Ladakh Intrusives at Kargil, northwestern Himalayas. Earth Planet. Sci. Lett. 44, 47-64.
Kocak, K., Isik, F., Arslan, M., Zedef, V., 2005. Petrological and source region characteristics of ophiolitic hornblende gabbros from the Aksaray and Kayseri regions, central Anatolian crystalline complex, Turkey. J. Asian Earth Sci. 25, 883-891.
La Touche, D., 1888. Rediscovery of Nummulites in Zanskar. Rec. Geol. Surv. India 21, 160-162.
Leech, M.L., Singh, S., Jain, A.K., 2007. Continuous metamorphic zircon growth and interpretation of U-Pb SHRIMP dating: An example from the western Himalaya. Int Geol Rev 49, 313-328.
Leech, M.L., Singh, S., Jain, A.K., Klemperer, S.L., Manickavasagam, R.M., 2005. The onset of India-Asia continental collision: Early, steep subduction required by the timing of UHP metamorphism in the western Himalaya. Earth Planet. Sci. Lett. 234, 83-97.
Li, Z.Y., Ding, L., Lippert, P.C., Song, P.P., Yue, Y.H., van Hinsbergen, D.J.J., 2016. Paleomagnetic constraints on the Mesozoic drift of the Lhasa terrane (Tibet) from Gondwana to Eurasia. Geology 44, 727-730.
Liu, D., Huang, Q., Fan, S., Zhang, L., Shi, R., Ding, L., 2014. Subduction of the Bangong-Nujiang Ocean: constraints from granites in the Bangong Co area, Tibet. Geol J 49, 188-206.
Liu, J.B., Aitchison, J.C., 2002. Upper Paleocene radiolarians from the Yamdrok melange, south Xizang (Tibet), China. Micropaleontology 48, 145-154.
Ludwig, K.R., 2003. Isoplot 3.00. A Geochronological Toolkit for Microsoft Excel. . Berkeley Geochronology Center, vol. 4, Berkeley, California. 70 pp.
Lydekker, R., 1880. Geology of Ladakh and neighbouring Districts. Record Geological Survey India 13, 26-59.
Lydekker, R., 1883. The geology of the Kashmir and Chamba territories and the districts of Khagan. Mem. Geol. Sur. Ind 22, 211-224.
MacMahon, C., 1901. Petrological notes on some peridotites, serpentines, gabbros, and associated rocks, from Ladakh, north-western Himalaya. Mere. Geol. Soc. India 31, 303-329.
Mahéo, G., Bertrand, H., Guillot, S., Villa, I.M., Keller, F., Capiez, P., 2004. The South Ladakh ophiolites (NW Himalaya, India): an intra-oceanic tholeiitic arc origin with implication for the closure of the Neo-Tethys. Chem. Geol. 203, 273-303.
Mahéo, G., Fayoux, X., Guillot, S., Garzanti, E., Capiez, P., Mascle, G., 2006. Relicts of an intra-oceanic arc in the Sapi-Shergol mélange zone (Ladakh, NW Himalaya, India): implications for the closure of the Neo-Tethys Ocean. J. Asian Earth Sci. 26, 695-707.
Malpas, J., Zhou, M.-F., Robinson, P.T., Reynolds, P.H., 2003. Geochemical and geochronological constraints on the origin and emplacement of the Yarlung Zangbo ophiolites, Southern Tibet. Geological Society, London, Special Publications 218, 191-206.

McDermid, I.R.C., Aitchison, J.C., Davis, A.M., Harrison, T.M., Grove, M., 2002. The Zedong terrane: a Late Jurassic intra-oceanic magmatic arc within the Yarlung-Tsangpo suture zone, southeastern Tibet. Chem. Geol. 187, 267-277.
Miller, C., Schuster, R., Klotzli, U., Frank, W., Purtscheller, F., 1999. Post-collisional potassic and ultrapotassic magmatism in SW Tibet: Geochemical and Sr-Nd-Pb-O isotopic constraints for mantle source characteristics and petrogenesis. J Petrol 40, 1399-1424.
Miller, C., Thoni, M., Frank, W., Schuster, R., Melcher, F., Meisel, T., Zanetti, A., 2003. Geochemistry and tectonomagmatic affinity of the Yungbwa ophiolite, SW Tibet. Lithos 66, 155-172.
Miyashiro, A., 1973. The Troodos ophiolitic complex was probably formed in an island arc. Earth Planet. Sci. Lett. 19, 218-224.
Miyashiro, A., 1975. Classification, Characteristics, and Origin of Ophiolites. Journal of Geology 83, 249-281.
Molnar, P., Tapponnier, P., 1975. Cenozoic Tectonics of Asia: Effects of a Continental Collision: Features of recent continental tectonics in Asia can be interpreted as results of the India-Eurasia collision. Science 189, 419-426.
Moores, E.M., Roeder, D.H., Abbas, S.G., Ahmad, Z., 1980. Geology and emplacement of the Muslim Bagh ophiolite complex, In: Panayiotou, A. (Ed.), Ophiolites; Proceedings, International ophiolite symposium. Cyprus Minist. Agric. Nat. Resour. Geol. Surv. Dep., Nicosia, Cyprus, pp. 424-429.
Najman, Y., Jenks, D., Godin, L., Boudagher-Fadel, M., Millar, I., Garzanti, E., Horstwood, M., Bracciali, L., 2017. The Tethyan Himalayan detrital record shows that India-Asia terminal collision occurred by 54 Ma in the Western Himalaya. Earth Planet. Sci. Lett. 459, 301-310.
Nicolas, A., Girardeau, J., Marcoux, J., Dupre, B., Wang, X.B., Cao, Y.G., Zheng, H.X., Xiao, X.C., 1981. The Xigaze Ophiolite (Tibet) - a Peculiar Oceanic Lithosphere. Nature 294, 414-417.
Paces, J.B., Miller, J.D., 1993. Precise U-Pb ages of Duluth complex and related mafic intrusions, northeastern Minnesota: Geochronological insights to physical, petrogenetic, paleomagnetic, and tectonomagmatic processes associated with the 1.1 Ga midcontinent rift system. Journal of Geophysical Research: Solid Earth 98, 13997-14013.
Pallister, J.S., Knight, R.J., 1981. Rare-earth element geochemistry of the Samail ophiolite near Ibra, Oman, In: Coleman Robert, G., Hopson Clifford, A. (Eds.), Oman ophiolite. American Geophysical Union, Washington, DC, United States, pp. 2673-2697.
Patchett, P.J., Kouvo, O., Hedge, C.E., Tatsumoto, M., 1982. Evolution of continental crust and mantle heterogeneity: evidence from Hf isotopes. Contrib Mineral Petr 78, 279-297.
Pearce, J.A., 1975. Basalt Geochemistry Used to Investigate Past Tectonic Environments on Cyprus. Tectonophysics 25, 41-67.
Pearce, J.A., 1982. Trace element characteristics of lavas from destructive plate boundaries, In: Thorpe, R.S. (Ed.), Orogenic andesites and related rocks. John Wiley and Sons, Chichester, England, pp. 528-548.

Pearce, J.A., 2008. Geochemical fingerprinting of oceanic basalts with applications to ophiolite classification and the search for Archean oceanic crust. Lithos 100, 14-48.
Pearce, J.A., Cann, J.R., 1973. Tectonic Setting of Basic Volcanic-Rocks Determined Using Trace-Element Analyses. Earth Planet. Sci. Lett. 19, 290-300.
Pearce, J.A., Robinson, P.T., 2010. The Troodos ophiolitic complex probably formed in a subduction initiation, slab edge setting. Gondwana Research 18, 60-81.
Pedersen, R.B., Searle, M.P., Corfield, R.I., 2001. U-Pb zircon ages from the Spontang Ophiolite, Ladakh Himalaya. J Geol Soc London 158, 513-520.
Ravikant, V., 2006. Utility of Rb-Sr geochronology in constraining Miocene and Cretaceous events in the eastern Karakoram, Ladakh, India. J. Asian Earth Sci. 27, 534-543.
Ravikant, V., Wu, F.Y., Ji, W.Q., 2009. Zircon U-Pb and Hf isotopic constraints on petrogenesis of the Cretaceous-Tertiary granites in eastern Karakoram and Ladakh, India. Lithos 110, 153-166.
Reibel, G., Reuber, I., 1982. The Peculiar Spongtang-Photaksar Ophiolitic Nappe (Ladakh, Himalaya). Cr Acad Sci Ii 294, 557-&.
Reichardt, H., Weinberg, R.F., Andersson, U.B., Fanning, C.M., 2010. Hybridization of granitic magmas in the source: The origin of the Karakoram Batholith, Ladakh, NW India. Lithos 116, 249-272.
Reuber, I., 1986. Geometry of Accretion and Oceanic Thrusting of the Spongtang Ophiolite, Ladakh-Himalaya. Nature 321, 592-596.
Reuber, I., 1989. The Dras Arc - 2 Successive Volcanic Events on Eroded Oceanic-Crust. Tectonophysics 161, 93-106.
Reuber, I., 1990. The Shyok ophiolite in Ladakh-Himalaya: relics of the Tethyan oceanic crust overlain by volcanosedimentary arc series of mid-Cretaceous age. Comptes Rendus, Academie des Sciences, Serie II 310, 1255-1262.
Reuber, I., Colchen, M., Mevel, C., 1992. The Spongtang ophiolite and ophiolitic melanges of the Zanskar, NW Himalaya, tracing the evolution of the closing Tethys in the Upper Cretaceous to the early Tertiary, In: Sinha, A.K. (Ed.), Himalayan orogen and global tectonics. Balkema; International Lithosphere Programme, Publication 197, pp. 235-266.
Reuber, I., Colchen, M., Mevel, C., 2015. The geodynamic evolution of the South-Tethyan, margin in Zanskar, NW-Himalaya, as revealed by the Spongtang ophiolitic melanges. Geodin Acta 1, 283-296.
Reuber, I., Montigny, R., Thuizat, R., Heitz, A., 1989. K-Ar Ages of Ophiolites and Arc Volcanics of the Indus Suture Zone - Clues on the Early Evolution of the Neo-Tethys. Eclogae Geol. Helv. 82, 699-715.
Rex, A.J., Searle, M.P., Tirrul, R., Crawford, M.B., Prior, D.J., Rex, D.C., Barnicoat, A.C., 1988. The geochemical and tectonic evolution of the central Karakoram, North Pakistan, In: Shackleton, R.M., Dewey, J.F., Windley, B.F. (Eds.), Tectonic evolution of the Himalayas and Tibet. Royal Society of London, London, United Kingdom, pp. 229-255.

Robertson, A., Degnan, P., 1994. The Dras Arc Complex - Lithofacies and Reconstruction of a Late Cretaceous Oceanic Volcanic Arc in the Indus Suture Zone, Ladakh-Himalaya. Sedimentary Geology 92, 117-145.
Robertson, A.H.F., Degnan, P.J., 1993. Sedimentology and Tectonic Implications of the Lamayuru Complex - Deep-Water Facies of the Indian Passive Margin, Indus Suture Zone, Ladakh Himalaya. Himalayan Tectonics 74, 299-321.
Rolland, Y., 2002. From intra-oceanic convergence to post-collisional evolution: example of the India-Asia convergence in NW Himalaya, from Cretaceous to present, In: Rosenbaum, G., Lister, G.S. (Eds.), Journal of the Virtual Explorer, pp. 185-208.
Russell, W., Papanastassiou, D., Tombrello, T., 1978. Ca isotope fractionation on the Earth and other solar system materials. Geochim Cosmochim Ac 42, 1075-1090.
Ryan, W.B.F., Carbotte, S.M., Coplan, J.O., O'Hara, S., Melkonian, A., Arko, R., Weissel, R.A., Ferrini, V., Goodwillie, A., Nitsche, F., Bonczkowski, J., Zemsky, R., 2009. Global Multi-Resolution Topography synthesis. Geochemistry, Geophysics, Geosystems 10, n/a-n/a.
Sarwar, G., 1992. Tectonic Setting of the Bela Ophiolites, Southern Pakistan. Tectonophysics 207, 359-381.
Searle, M., Corfield, R.I., Stephenson, B., McCarron, J., 1997. Structure of the North Indian continental margin in the Ladakh-Zanskar Himalayas: Implications for the timing of obduction of the Spontang ophiolite, India-Asia collision and deformation events in the Himalaya. Geological Magazine 134, 297-316.
Searle, M., Cox, J., 1999. Tectonic setting, origin, and obduction of the Oman ophiolite. Geol. Soc. Am. Bull. 111, 104-122.
Searle, M., Khan, M.A., Fraser, J., Gough, S., Jan, M.Q., 1999. The tectonic evolution of the Kohistan-Karakoram collision belt along the Karakoram Highway transect, north Pakistan. Tectonics 18, 929-949.
Searle, M.P., 1986. Structural Evolution and Sequence of Thrusting in the High Himalayan, Tibetan-Tethys and Indus Suture Zones of Zanskar and Ladakh, Western Himalaya. Journal of Structural Geology 8, 923-+.
Searle, M.P., Cooper, D.J.W., Rex, A.J., 1988. Collision Tectonics of the Ladakh Zanskar Himalaya. Philosophical Transactions of the Royal Society a-Mathematical Physical and Engineering Sciences 326, 117-+.
Searle, M.P., Parrish, R.R., Tirrul, R., Rex, D.C., 1990a. Age of crystallization and cooling of the K2 gneiss in the Baltoro Karakoram. Journal of the Geological Society, London 147, 603-606.
Searle, M.P., Pickering, K.T., Cooper, D.J.W., 1990b. Restoration and evolution of the intermontane Indus molasse basin, Ladakh Himalaya, India. Tectonophysics 174, 301-314.
Searle, M.P., Tirrul, R., 1991. Structural and thermal evolution of the Karakoram crust. Journal of the Geological Society, London 148, 65-82.
Searle, M.P., Warren, C.J., Waters, D.J., Parrish, R.R., 2003. Subduction zone polarity in the Oman Mountains: Implications for ophiolite emplacement. Ophiolites in Earth History 218, 467-480.

Searle, M.P., Weinberg, R.F., Dunlap, W.J., 1998. Transpressional tectonics along the Karakoram fault zone, northern Ladakh: constraints on Tibetan extrusion, In: Holdsworth, R.E., Strachan, R.E., Dewey John, F. (Eds.), Continental Transpressional and Transtensional Tectonics. Geological Society, London, pp. 307–326.
Seton, M., Müller, R.D., Zahirovic, S., Gaina, C., Torsvik, T., Shephard, G., Talsma, A., Gurnis, M., Turner, M., Maus, S., Chandler, M., 2012. Global continental and ocean basin reconstructions since 200 Ma. Earth-Science Reviews 113, 212-270.
Shellnutt, J.G., Lee, T.Y., Brookfield, M.E., Chung, S.L., 2014. Correlation between magmatism of the Ladakh Batholith and plate convergence rates during the India-Eurasia collision. Gondwana Research 26, 1051-1059.
Shervais, J.W., 1982. Ti-V Plots and the Petrogenesis of Modern and Ophiolitic Lavas. Earth Planet. Sci. Lett. 59, 101-118.
Sinclair, H.D., Jaffey, N., 2001. Sedimentology of the Indus Group, Ladakh, northern India: implications for the timing of initiation of the palaeo-Indus River. J Geol Soc London 158, 151-162.
Singh, S., Kumar, R., Barley, M.E., Jain, A.K., 2007. SHRIMP U-Pb ages and depth of emplacement of Ladakh Batholith, Eastern Ladakh, India. J. Asian Earth Sci. 30, 490-503.
St-Onge, M.R., Rayner, N., Palin, R.M., Searle, M.P., Waters, D.J., 2013. Integrated pressure-temperature-time constraints for the Tso Morari dome (Northwest India): implications for the burial and exhumation path of UHP units in the western Himalaya. Journal of Metamorphic Geology 31, 469-504.
Stampfli, G.M., Borel, G.D., 2002. A plate tectonic model for the Paleozoic and Mesozoic constrained by dynamic plate boundaries and restored synthetic oceanic isochrons. Earth Planet. Sci. Lett. 196, 17-33.
Steck, A., 2003. Geology of the NW Indian Himalaya. Eclogae Geol. Helv. 96, 147-U113.
Steck, A., Spring, L., Vannay, J.C., Masson, H., Bucher, H., Stutz, E., Marchant, R., Tieche, J.C., 1993. The tectonic evolution of the northwestern Himalaya in eastern Ladakh and Lahul, India, In: Treloar, J ; Searle (Eds.), Himalayan tectonics. Geological Society of London, London, United Kingdom, pp. 265-276.
Stern, R.J., 2004. Subduction initiation: spontaneous and induced. Earth Planet. Sci. Lett. 226, 275-292.
Sterne, E.J., 1979. Report on geological traverses across the Indus-Tsangpo suture zone in Ladakh, northern India. Harvard University.
Sun, S.S., McDonough, W.F., 1989. Chemical and isotopic systematics of oceanic basalts: implications for mantle composition and processes. Geological Society, London, Special Publications 42, 313-345.
Tewari, A., 1964. On the Upper Tertiary deposits of Ladakh Himalayas and correlation of various geotectonic units of Ladakh with those of the Kumaon-Tibet Region. Geol. Congr. New Delhi, Sect. ll, 37-58.

Thirlwall, M.F., Anczkiewicz, R., 2004. Multidynamic isotope ratio analysis using MC-ICP-MS and the causes of secular drift in Hf, Nd and Pb isotope ratios. International Journal of Mass Spectrometry 235, 59-81.
Vadlamani, R., Guha, D., 2002. Ultrapotassic post-collisional dyke from the Ladakh batholith, Northwest Himalaya. J Geol Soc India 59, 473-476.
Vervoort, J.D., Patchett, P.J., Söderlund, U., Baker, M., 2004. Isotopic composition of Yb and the determination of Lu concentrations and Lu/Hf ratios by isotope dilution using MC-ICPMS. Geochemistry, Geophysics, Geosystems 5.
Wang, C.S., Liu, Z.F., others, 1999. Xigaze forearc basin and Yarlung Zangbo suture zone, Tibet. Geological Publishing House, Beijing.
Wang, J.G., Hu, X.M., Garzanti, E., An, W., Liu, X.C., 2017. The birth of the Xigaze forearc basin in southern Tibet. Earth Planet. Sci. Lett. 465, 38-47.
Wang, X.B., Bao, P.S., Xiao, X.C., 1987. Ophiolites of the Yarlung Zangbo (Tsangbo) River, Xizang (Tibet). Publishing House of Surveying and Mapping. 118 pp. plus foldout Geological Map of the Ophioilte Zone along the Middle Yarlung Zangbo (Tsangbo) River, Xizang (Tibet), Beijing.
Weinberg, R.F., Dunlap, W.J., 2000. Growth and Deformation of the Ladakh Batholith, Northwest Himalayas: Implications for Timing of Continental Collision and Origin of Calc-Alkaline Batholiths. J Geol 108, 303-320.
Whattam, S.A., Stern, R.J., 2011. The 'subduction initiation rule': a key for linking ophiolites, intra-oceanic forearcs, and subduction initiation. Contrib Mineral Petr 162, 1031-1045.
White, L.T., Ahmad, T., Ireland, T.R., Lister, G.S., Forster, M.A., 2011. Deconvolving episodic age spectra from zircons of the Ladakh Batholith, northwest Indian Himalaya. Chem. Geol. 289, 179-196.
Williams, I.S., 1998. U-Th-Pb geochronology by ion microprobe. Reviews in Economic Geology 7, 1-35.
Winchester, J.A., Floyd, P.A., 1977. Geochemical discrimination of different magma series and their differentiation products using immobile elements. Chem. Geol. 20, 325-343.
Wood, D.A., 1980. The application of a ThHfTa diagram to problems of tectonomagmatic classification and to establishing the nature of crustal contamination of basaltic lavas of the British Tertiary Volcanic Province. Earth Planet. Sci. Lett. 50, 11-30.
Woodhead, J., Hergt, J., Shelley, M., Eggins, S., Kemp, R., 2004. Zircon Hf-isotope analysis with an excimer laser, depth profiling, ablation of complex geometries, and concomitant age estimation. Chem. Geol. 209, 121-135.
Xia, B., Yu, H.X., Chen, G.W., Qi, L., Zhao, T.P., Zhou, M.F., 2003. Geochemistry and tectonic environment of the Dagzhuka ophiolite in the Yarlung-Zangbo suture zone, Tibet. Geochem J 37, 311-324.
Yang, T.S., Ma, Y.M., Zhang, S.H., Bian, W.W., Yang, Z.Y., Wu, H.C., Li, H.Y., Chen, W.W., Ding, J.K., 2015. New insights into the India-Asia collision process from Cretaceous paleomagnetic and geochronologic results in the Lhasa terrane. Gondwana Research 28, 625-641.

Zahirovic, S., Muller, R.D., Seton, M., Flament, N., Gurnis, M., Whittaker, J., 2012. Insights on the kinematics of the India-Eurasia collision from global geodynamic models. Geochem Geophy Geosy 13.
Zaigham, N.A., Mallick, K.A., 2000. Bela ophiolite zone of southern Pakistan: Tectonic setting and associated mineral deposits. Geol. Soc. Am. Bull. 112, 478-489.
Zhou, M.F., Robinson, P.T., Malpas, J., Li, Z.J., 1996. Podiform chromitites in the Luobusa ophiolite (southern Tibet): Implications for melt-rock interaction and chromite segregation in the upper mantle. J Petrol 37, 3-21.
Zhou, Y.N., Cheng, X., Yu, L., Yang, X.F., Su, H.L., Peng, X.M., Xue, Y.K., Li, Y.Y., Ye, Y.K., Zhang, J., Li, Y.Y., Wu, H.N., 2016. Paleomagnetic study on the Triassic rocks from the Lhasa Terrane, Tibet, and its paleogeographic implications. J. Asian Earth Sci. 121, 108-119.
Zyabrev, S.V., Kojima, S., Ahmad, T., 2008. Radiolarian biostratigraphic constraints on the generation of the Nidar ophiolite and the onset of Dras arc volcanism: Tracing the evolution of the closing Tethys along the Indus – Yarlung-Tsangpo suture. Stratigraphy 5, 99-112.

Biographies

Solomon Buckman is a Senior Lecturer in economic and field geology at the School of Earth and Environmental Sciences at the University of Wollongong in Australia. Prior to that he was a geology lecturer at the University of South Australia. He undertook a post-doc position

at James Cook University investigating the Cannington Ag-Pb-Zn deposit after completing his PhD at the University of Hong Kong in 2000, which was a study of the tectonic evolution of West Junggar within the Central Asian Orogenic Belt of NW China. Solomon worked as an exploration geologist across Australia for two years after completing his B.Sc. (Hons) at the University of Sydney in 1993. He is a field geologist with interests and expertise in the tectonic evolution of ophiolites and island arcs in eastern Australia (New England and Lachlan orogens), the Himalayas, China and South America. His interests are in convergent margin tectonics and in particular, mechanisms of continental growth involving the addition of juvenile, oceanic terranes to continental margins.

Jonathan C. Aitchison is Professor and Head of the School of Earth and Environmental Sciences at The University of Queensland, Australia. Prior to that he was at The University of Sydney and the University of Hong Kong. He received his PhD from the University of New England, NSW Australia in 1989 and studied for his BSc (Hons) and MSc at the University of Otago in New Zealand and studied in Japan at Niigata and Kochi universities. His research interests include the evolution of convergent plate margins and collisional orogens especially arc-continent collisions worldwide. In particular, he has concentrated on the SW Pacific, Japan, eastern Australia, New Caledonia and the Philippines. His primary interest is the India-Asia collision particularly in Tibet, where he has worked for

two decades. As an additional research theme, he also works on radiolarians to provide the biostratigraphic age constraints necessary for unravelling wicked tectonic problems.

Allen Nutman is a professor and current head of school at the University of Wollongong. He works mostly on early Precambrian basement rocks of Greenland, Australia, China, Brazil and Russia with occasional excursions into the Phanerozoic orogens of eastern Australia. He integrates his own mapping and field observations with U-Pb zircon geochronology. He has 25 years of experience working on SHRIMP ion microprobe U-Pb geochronology on 8 different instruments (I, IIs and RG) in Australia, China, Japan and

Korea. His research interests include evolution of the Eoarchaean Earth and the appearance of earliest life.

Vickie C. Bennett is a professor and associate director at the Research School of Earth Sciences, the Australian National University, Canberra, Australia and head of the SPIDE^{2}R isotope laboratory. Her research focuses on the development and application of radiogenic isotopic methods to understanding the origin and evolution of Earth's continental crust and mantle reservoirs, early planetary differentiation, and geosphere–biosphere interactions in deep time. She is co-editor of the 1st (2007) and 2ed (2018) editions of the major reference

book “Earth’s Oldest Rocks”. Bennett is a Geochemical Fellow and a Fellow of the Geological Society of America and is currently Vice-President (President-elect) of the Geochemical Society.

Wanchese M. Saktura is a PhD candidate at University of Wollongong, Australia. He obtained B.Sc. (Adv) Honours 1st Class for his research on tectonic evolution of the Beishan Orogen, China. His current research is focused on the Himalayan Orogeny, more precisely,

tectonic accretionary processes and paleogeography along Tethyan oceans prior to the final continent-continent collision. Additional interests include application of thermochronology in orogenic settings, especially, use of optically stimulated luminescence (OSL) technique in geology to understand most recent neotectonic processes and evolution of mountainous relief.

Jessica M. J. Walsh completed a Bachelor of Science (Honours) at the University of Wollongong (UOW), Australia in 2015, which focused on multiple magmatic related Mo-Cu systems in the Qinling Orogenic Belt, Central China. She is currently completing her PhD at the same institute, with her research focusing on the geotectonic evolution of the Himalaya, with specific reference to arc-continent collision prior to final continent-continent collision of India and Eurasia. Broadly, her research interests include tectonic evolution of orogenic belts and continental growth processes.

Sarah Kachovich is a PhD candidate at The University of Queensland. She specialises in radiolarian biostratigraphy, with her research focusing on linking microfossils to tectonic

problems, such as the Himalayan collision and the tectonic evolution of the New England Orogen, eastern Australia.

Prof. Hiroshi Hidaka is a foundation researcher of the Hiroshima SHRIMP group – the first SHRIMP large ionmicroprobe instrument to be sold outside of Australia and which was installed in 1997. He is an isotope geochemist with a wide range of interests, both from the perspective of geology and also nuclear science. Concerning the latter, he has worked extensively on the natural (Palaeoproterozoic) nuclear reactor from Oklo in West Africa. In this, his studies involve both the use of conventional IDTIMS methods and the use of

SHRIMP to document the distribution of fission products on the mineral-grain scale. From the geological perspective he has undertaken extensive U-Pb zircon dating using SHRIMP, both on Japanese projects and in collaboration with overseas researchers. One overseas link has been with co-author on this paper Allen Nutman, mostly investigating early crustal evolution via ancient rocks in Greenland. Prof Hidaka is currently a faculty member at Nagoya University.

Table 4– whole rock geochemistry

ample	BST 08	BST 09	BST 01	BST 04	BST 07	BST 02	BST 03	BST 15	BST 22	BST 19	BST 11	BST 16	BST 17	BST 06	BST 18	BST 05	BST20
ocktype	asalt	asalt	asalt	asalt	asalt	asalt	asalt	asalt dyke	asalt	abbro	abbro	abbro	abbro	abbro	abbro	abbro	abbro egmatite
atitude (N)	4.05675	4.05675	4.051733	4.051733	4.05675	4.051733	4.051733	4.05997	4.06513	4.05997	4.06214	4.05997	4.05997	4.05465	4.05997	4.05277	4.05997
ongitude (E)	6.77718	6.77718	6.771300	6.771300	6.77718	6.771300	6.771300	6.77534	6.77939	6.77534	6.78197	6.77534	6.77534	6.77379	6.77534	6.77240	6.77534
	Majors (%)																
iO_2	6.60	6.84	6.86	7.02	7.04	8.65	8.99	2.69	2.16	6.63	6.94	0.52	1.18	2.37	3.11	4.29	5.67
iO_2	.59	.96	.94	.49	.33	.69	.71	.97	.74	.35	.25	.73	.01	.60	.80	.87	.15
l_2O_3	5.13	4.18	5.96	5.03	5.58	5.77	7.35	4.69	9.37	5.88	6.02	4.66	4.53	5.09	4.97	5.76	7.86

e_2O_3	1.83	1.34	1.55	.47	.77	.20	2.62	2.18	.60	.08	.55	1.24	3.81	0.69	0.11	0.63	.29
nO	.18	.19	.24	.14	.15	.14	.15	.18	.13	.12	.14	.18	.19	.18	.15	.16	.02
gO	.59	.12	.10	.07	.02	.10	.71	.26	.84	1.13	.92	.36	.38	.46	.47	.38	.85
aO	1.00	.56	.45	0.68	0.27	0.16	.19	.05	.89	3.83	.89	.27	.47	0.03	.15	.74	3.87
a_2O	.34	.97	.38	.48	.50	.79	.99	.52	.32	.96	.93	.52	.88	.91	.49	.24	.84
$_2O$	.20	.12	.83	.13	.10	.28	.41	.62	.96	.65	.25	.32	.31	.84	.18	.23	.42
$_2O_5$	.17	.25	.26	.15	.17	.18	.19	.09	.25	.05	.15	.06	.07	.07	.08	.08	.01
O_3	.22	.23	.00	.02	.04	.02	0.01	.01	.04	.01	.01	.00	.01	.00	0.01	0.01	0.01
OI	.21	.44	.43	.54	.44	.36	.01	.85	.11	.2	.32	.16	.53	.08	.56	.1	.29
otal	**00.06**	**00.06**	**00.00**	**00.22**	**9.43**	**00.34**	**9.32**	**00.10**	**9.43**	**9.43**	**00.36**	**00.01**	**00.37**	**00.32**	**00.06**	**9.47**	**9.47**
	Trace elements (ppm)																
a	9.4	7.8	6.1	1	4.8	7	6.4	8	00	5.5	7	3.8	6.3	27	5.7	8.2	2.6

e	03	9.9	7.9	0.6	0.3	2.1	1.7	.9	99	.2	3.9	.7	43	.3	.7	.5	.2
r	50	10	20	50	20	60	90	0	0	60	90	00	0	0	50	0	0
s	.24	.29	.6	.09	.15	.17	.29	.08	5.05	.24	.13	.13	.29	.56	.06	.06	.11
y	.34	.23	.85	.03	.42	.27	.47	.43	.15	.47	.92	.89	.94	.87	.39	.42	.87
r	.61	.89	.73	.4	.88	.37	.06	.26	.59	.69	.53	.06	.03	.07	.24	.4	.76
u	.26	.57	.6	.27	.22	.26	.47	.85	.74	.55	.99	.64	.76	.55	.73	.76	.2
a	7.1	7	7.4	5.9	6.9	5.4	5.3	6.5	8.1	2.9	4.1	4.9	8	4	5.4	6.3	0.9
d	.76	.62	.22	.53	.08	.62	.7	.95	.13	.05	.63	.52	.28	.26	.66	.9	.59
f	.8	.4	.1	.5	.2	.8	.6	.7	9.2	.5	.9	.4	.8	.1	.6	.6	.2
o	.19	.35	.29	.13	.99	.16	.4	.82	.59	.56	.9	.68	.66	.64	.77	.77	.22
a	.3	.3	.7	.3	.5	.9	.8	.3	7.1	.4	.6	.9	.6	.5	.9	.3	.7
u	.49	.56	.56	.48	.4	.5	.55	.38	.25	.24	.35	.3	.33	.33	.36	.37	.11
b	.8	.1	.3	.2	.1	.6	.5	.3	29	.4			.9	.8		.2	.2
d	.9	3.1	3.1	.5	.3	0.1	1.4	.5	0.4	.9	.6	.6	.8	.9	.1	.5	.7

r	.69	.66	.61	.78	.63	.95	.23		.69	.82	.48	.85	.71	.67	.95	.03	.12
b	.6	.3	8.3	.4	.6		.1	.2	25	.2			.6	.3	.9	.5	1.3
m	.03	.31	.04	.16	.83	.52	.74	.99	.06	.27	.74	.57	.41	.49	.81	.94	.24
n	82								86		0		66				
r	16.5	63.5	21	2.7	49.5	9.9	7.3	78	21	66	37.5	7.5	35.5	5.9	59	00.5	9.9
a	.1	.2	.5	.2	.2	.3	.2	.1	3.4	.1	.2	.1	.1	.1	.1	.1	0.1
b	.86	.03	.96	.85	.73	.89	.04	.53	.64	.37	.66	.46	.44	.42	.52	.54	.12
h	.15	.23	.57	.16	.17	.17	.2	.15	6.2	.2	.2	.12	.19	.15	.13	.14	0.05
m	.52	.59	.58	.52	.44	.52	.6	.37	.25	.26	.38	.3	.33	.33	.34	.34	.13
	.09	.1	.19	.07	.08	.08	.17	.09	.57	.05	.11	.08	.11	.1	.09	.08	0.05
	93	98	29	78	77	03	90	75	1	01	22	10	30	45	12	96	41
	1		1	1			1		1		1					1	
	3.7	9.1	6.2	1.7	8.7	3.1	2.4	1.7	3.7	5.9	4.8	9.3	8.7	9.2	1.8	2.4	.5
b	.24	.61	.47	.04	.75	.18	.71	.36	.61	.42	.3	.92	.02	.93	.27	.31	.71

r	16	52	22	6	9	07	01	7	170	8	3	8	5	6	5	7	

Table 5– U-Pb SHRIMP data

abels	ite	/ppm	h/ppm	h/U	f206	$^{238}U/^{206}Pb$(meas)			$^{207}Pb/^{206}Pb$(meas)			age $^{206}Pb/^{238}U$(corr)		
BST-12														
.1	,osc,eq	75	24	.13	.85	6.33		.27	.0556		.0017	36.5		.7
.1	,osc/h,fr	88	75	.93	.29	7.23		.10	.0619		.0022	32.0		.0
.1	,osc/h,eq	48	37	.97	.10	6.38		.80	.0556		.0015	36.0		.0
.1	,osc,eq	83	39	.58	.43	6.36		.59	.0520		.0009	37.0		.4
.1	,osc,eq,fr	13	28	.05	.95	5.74		.03	.0564		.0015	38.1		.5
.1	,osc,p,fr	92	76	.64	.43	7.80		.85	.0523		.0012	32.9		.9
.1	,osc/h,eq,fr	09	27	.78	.30	7.18		.45	.0511		.0013	34.8		.4
.1	,osc,p,fr	42	29	.55	.73	6.56		.76	.0544		.0017	36.0		.7
.1	,osc,p,fr	17	01	.93	.78	6.00		.94	.0626		.0021	36.2		.1

0.1	,osc/h,p	66	74	.54	.42	7.06		.73	.0523		.0011	35.0		.6
1.1	,h,p	96	38	.88	.33	7.82		.94	.0510		.0013	33.0		.2
2.1	,h,p	61	56	.99	.41	5.46		.78	.0521		.0011	39.7		.8
BST-05														
.1	iny,h/osc	46	026	.39	.26	7.36		.96	.0585		.0035	33.0		.5
.1	iny,h/osc	105	807	.54	.83	7.94		.11	.0550		.0016	32.0		.2
.1	iny,h/osc	383	802	.09	.21	4.81		.48	.0530		.0014	42.0		.5
.1	iny,h/osc	488	853	.60	.11	7.46		.22	.0568		.0014	10.0		.0

isotopic ratios uncorrected for common Pb

Spot: x.y = grain followed by analysis number

Site: m = middle, e = end, p = prismatic grain, eq=equant grain, osc = oscillatory zoned, h = homogeneous, fr = fragment

%f206: percentage of ^{206}Pb that is non-radiogenic (common)

ages corrected for common Pb by the '207' method (modelled as concordant)

all analytical errors are 1 sigma

Table 6 Hf data

				Measured			ε_{Hf}(0)			-Pb	initial			
nalysis	$^{176}Lu/^{177}Hf$			$^{176}Hf/^{177}Hf$			in run errors only			age (Ma)	$^{176}Hf/^{177}Hf$	$_{Hf}(t)$		SE
.1	.00328		.00003	.28313		.00001	2.11		.40	36.5	0.28312	4.9		.8
.1	.00639		.00001	.28319		.00002	4.37		.60	32	0.28318	6.8		.20
.1	.00595		.00011	.28317		.00001	3.61		.49	36	0.28315	6.1		.0
.1	.00544		.00009	.28315		.00001	3.09		.51	37	0.28314	5.6		.0
.1	.00571		.00001	.28320		.00001	4.91		.44	38.1	0.28319	7.5		.9
.1	.00585		.00006	.28313		.00001	2.14		.48	32.9	0.28311	4.6		.0
.1	.00402		.00001	.28320		.00001	4.66		.45	34.8	0.28319	7.3		.0
.1	.00285		.00006	.28315		.00001	2.97		.39	36	0.28314	5.7		.8

0.1	.00738		.00001	.28320		.00002	4.70		.59	36.2	0 .28318	7.1		.2
1.1	.00668		.00002	.28315		.00001	2.98		.52	35	0 .28314	5.4		.0
2.1	.00369		.00006	.28315		.00001	2.91		.42	33	0 .28314	5.5		.8
	.01245		.00039	.28313		.00002	2.36		.70	37	0 .28310	4.3		.4
	.00675		.00007	.28325		.00003	6.45		.93	37	0 .28323	8.9		.8
	.00344		.00007	.28319		.00002	4.37		.69	37	0 .28318	7.1		.4
	.00517		.00007	.28319		.00001	4.36		.48	37	0 .28318	6.9		.0
	.00551		.00004	.28314		.00001	2.73		.43	37	0 .28313	5.3		.9
	.00355		.00006	.28315		.00001	2.81		.39	37	0 .28314	5.5		.8

	.00648		.00004	.28318		.00001	4.07		.47	37	.28317	0 6.5		.0

[1] Initial ratios are calculated at either the SHRIMP U-Pb age (Table 2) or at the average age of 137 Ma. Uncertainty in initial ratios are given as 2 SE.

[2] εHf values are calculated using CHUR parameters given in Bouvier et al, 2008.

Highlights for Spongtang manuscript

- New U-Pb zircon (SHRIMP) age of gabbros from Spongtang ophiolite yield age of ~136 Ma which contrasts with previous age of ~177 Ma reported by Pedersen et al., 2001.
- Initial ε_{Hf} zircon values of +14 to +16, indicate Early Cretaceous juvenile, depleted mantle sources devoid of contamination by older continental crust
- Petrology and geochronology both indicate development of the Early Cretaceous Spong Arc is superimposed on older Jurassic N-MORB crust
- The age, composition and nature of geological relationships with the underlying Indian rocks indicates the Spong Arc was a juvenile, intra-oceanic terrane that first collided with India before the onset of final continent-continent collision

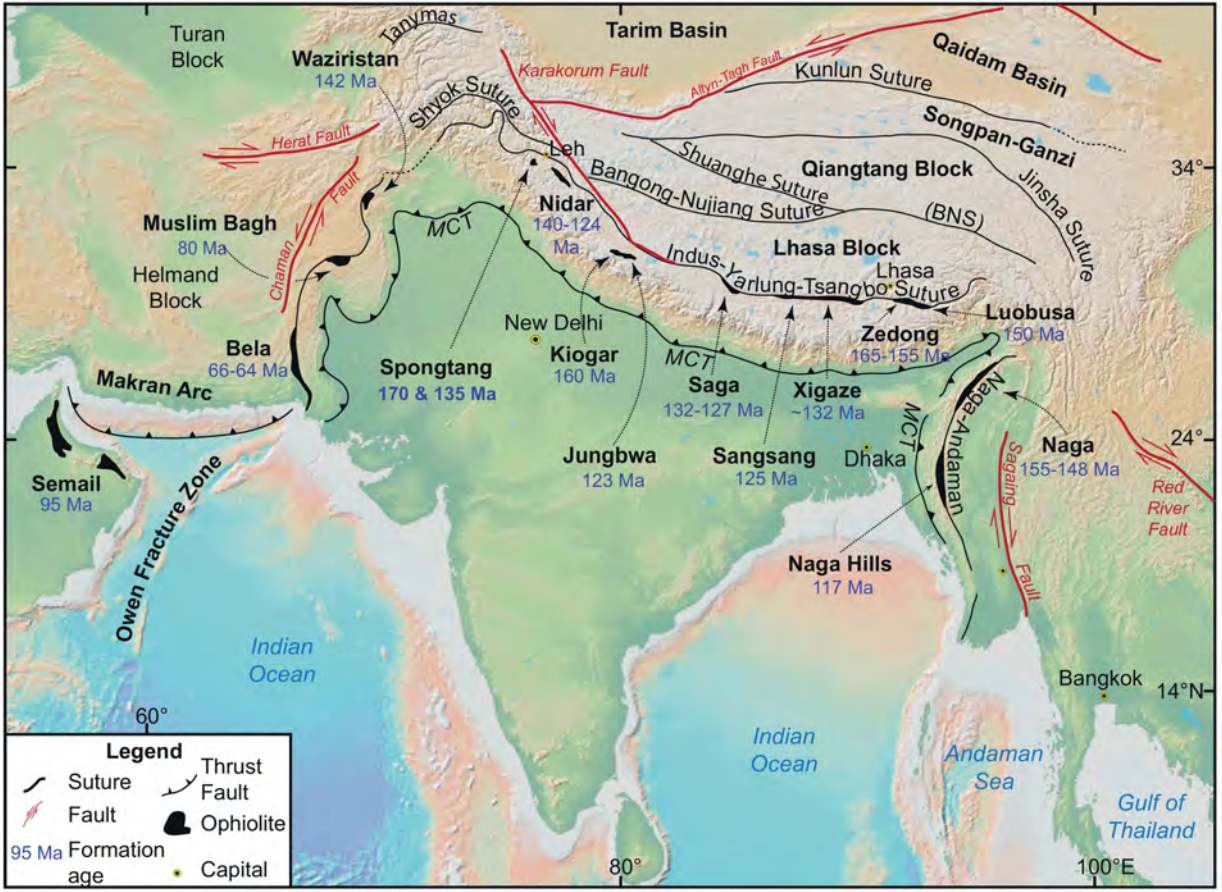
Turan Block
Waziristan
142 Ma
Tanymas
Tarim Basin
Karakorum Fault
Altyn-Tagh Fault
Qaidam Basin
Kunlun Suture
Songpan-Ganzi
Shyok Suture
Herat Fault
Leh
Shuanghe Suture
Qiangtang Block
Jinsha Suture
34°
Bangong-Nujiang Suture
(BNS)
Nidar
140-124 Ma
Muslim Bagh
80 Ma
Chaman Fault
MCT
Lhasa Block
Indus-Yarlung-Tsangbo Suture
Lhasa
Helmand Block
New Delhi
Luobusa
150 Ma
Zedong
165-155 Ma
Bela
66-64 Ma
Kiogar
160 Ma
MCT
Spongtang
170 & 135 Ma
Saga
132-127 Ma
Xigaze
~132 Ma
Naga-Andaman
Makran Arc
Jungbwa
123 Ma
Sangsang
125 Ma
Dhaka
MCT
Naga
155-148 Ma
24°
Sagaing Fault
Red River Fault
Semail
95 Ma
Owen Fracture Zone
Naga Hills
117 Ma
Indian Ocean
Bangkok
14°N
60°
Indian Ocean
Andaman Sea
Gulf of Thailand
80°
100°E
Legend
Suture
Thrust Fault
Fault
Ophiolite
95 Ma Formation age
Capital

Figure 1

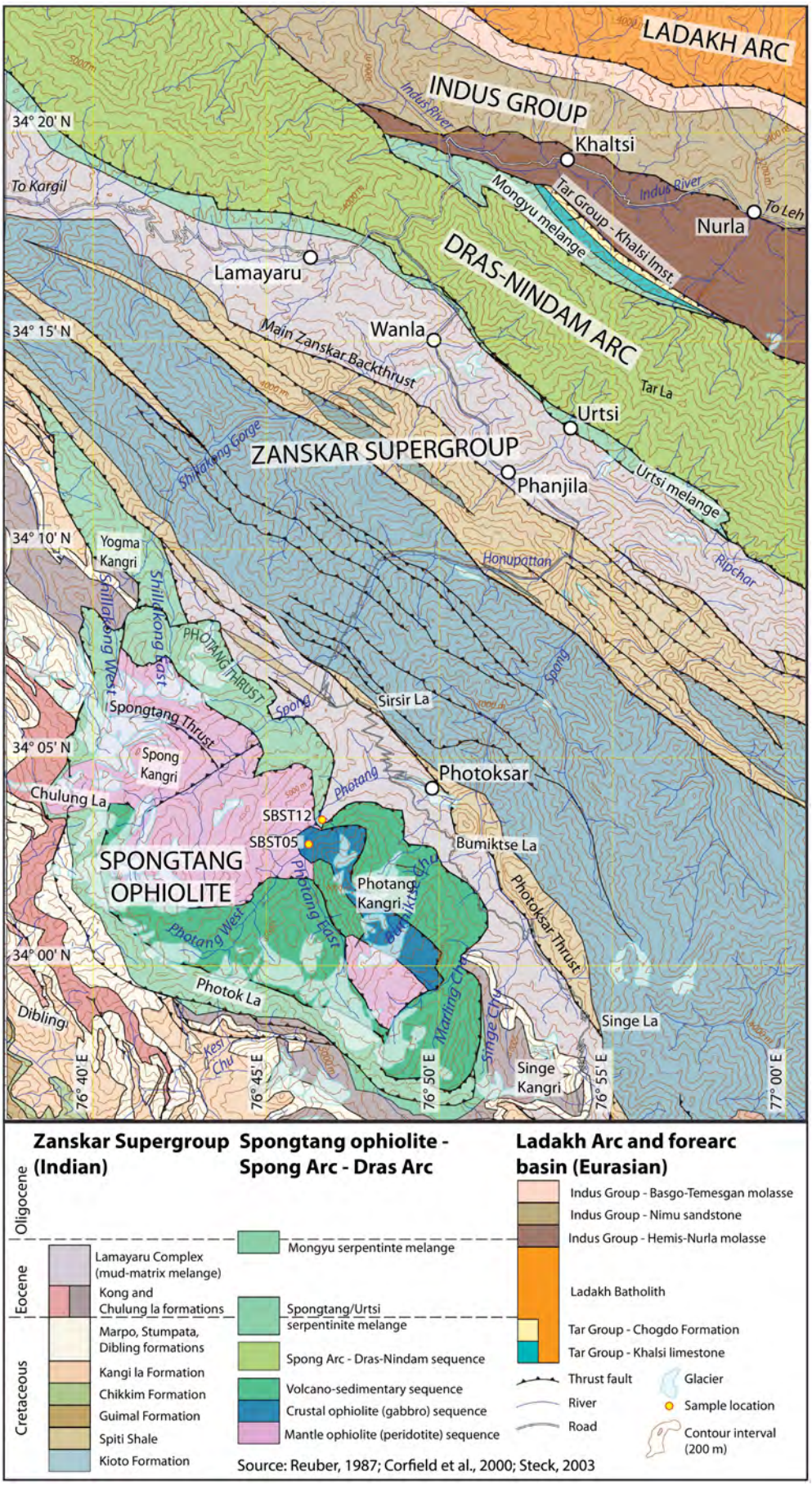
LADAKH ARC
INDUS GROUP
Indus River
Khaltsi
34° 20' N
To Kargil
Tar Group - Khalsi lmst.
Mongyu melange
Nurla
To Leh
Lamayaru
DRAS-NINDAM ARC
34° 15' N
Wanla
Main Zanskar Backthrust
Tar La
Urtsi
ZANSKAR SUPERGROUP
Shilakong Gorge
Phanjila
Urtsi melange
34° 10' N
Yogma Kangri
Honupattan
Ripchar
Shillakong West
Shillakong East
PHOTANG THRUST
Spong
Spongtang Thrust
Sirsir La
34° 05' N
Spong Kangri
Photoksar
Photang
Chulung La
SBST12
SBST05
Bumiktse La
SPONGTANG OPHIOLITE
Photang Kangri
Photang West
Photang East
Bumiktse Chu
Photoksar Thrust
34° 00' N
Photok La
Dibling
Marling Chu
Singe Chu
Singe La
Kesi Chu
Singe Kangri
76° 40' E
76° 45' E
76° 50' E
76° 55' E
77° 00' E
Zanskar Supergroup (Indian)
Oligocene
Eocene
Cretaceous
Lamayaru Complex (mud-matrix melange)
Kong and Chulung la formations
Marpo, Stumpata, Dibling formations
Kangi la Formation
Chikkim Formation
Guimal Formation
Spiti Shale
Kioto Formation
Spongtang ophiolite - Spong Arc - Dras Arc
Mongyu serpentinte melange
Spongtang/Urtsi serpentinite melange
Spong Arc - Dras-Nindam sequence
Volcano-sedimentary sequence
Crustal ophiolite (gabbro) sequence
Mantle ophiolite (peridotite) sequence
Ladakh Arc and forearc basin (Eurasian)
Indus Group - Basgo-Temesgan molasse
Indus Group - Nimu sandstone
Indus Group - Hemis-Nurla molasse
Ladakh Batholith
Tar Group - Chogdo Formation
Tar Group - Khalsi limestone
Thrust fault
River
Road
Glacier
Sample location
Contour interval (200 m)
Source: Reuber, 1987; Corfield et al., 2000; Steck, 2003

Figure 2

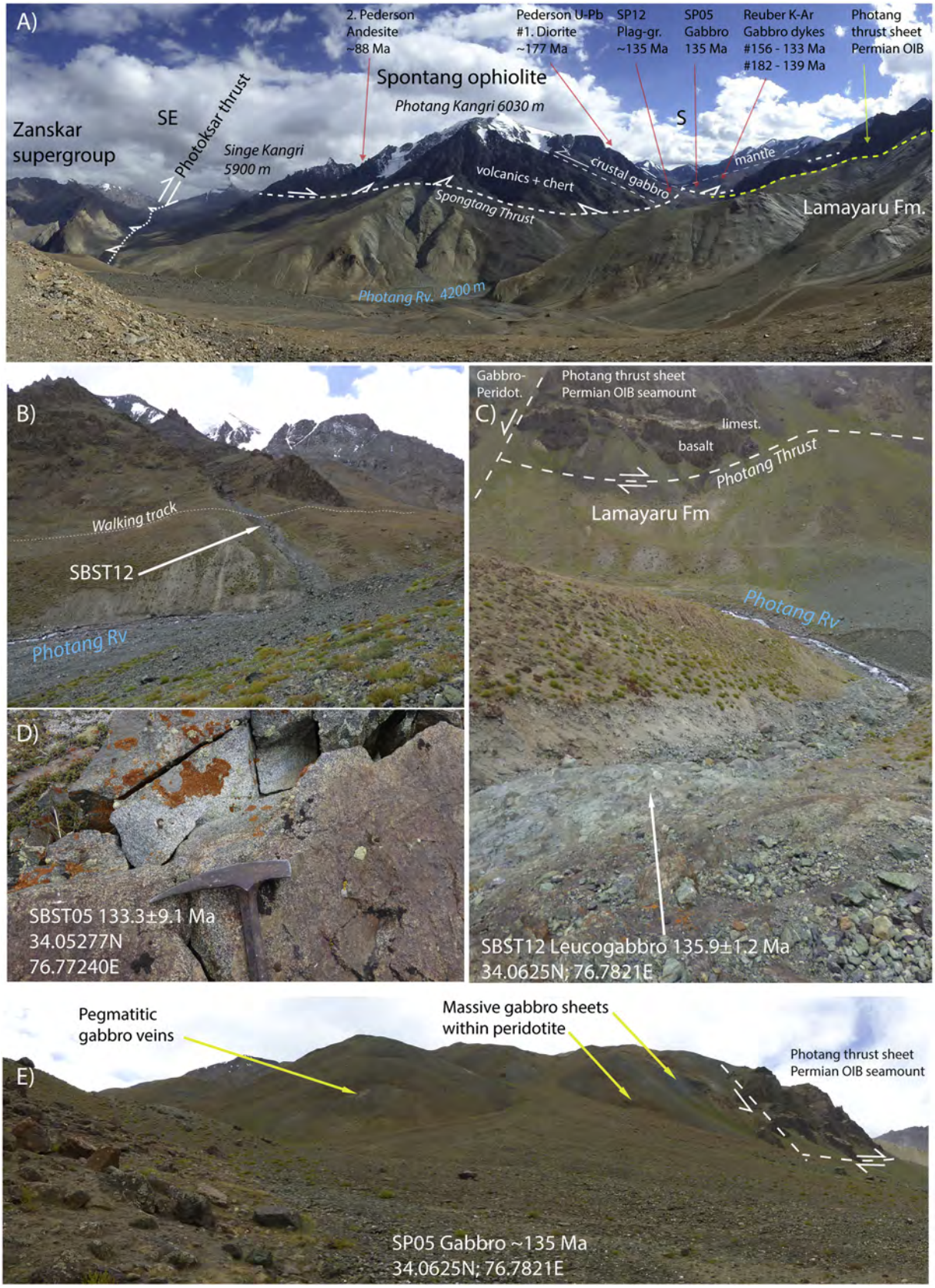
A)
2. Pederson
Andesite
~88 Ma
Pederson U-Pb
#1. Diorite
~177 Ma
SP12
Plag-gr.
~135 Ma
SP05
Gabbro
135 Ma
Reuber K-Ar
Gabbro dykes
#156 - 133 Ma
#182 - 139 Ma
Photang
thrust sheet
Permian OIB
Spontang ophiolite
Photang Kangri 6030 m
Zanskar
supergroup
SE
Photoksar thrust
Singe Kangri
5900 m
S
mantle
crustal gabbro
volcanics + chert
Spongtang Thrust
Lamayaru Fm.
Photang Rv. 4200 m
B)
Walking track
SBST12
Photang Rv
C)
Gabbro-
Peridot.
Photang thrust sheet
Permian OIB seamount
limest.
basalt
Photang Thrust
Lamayaru Fm
Photang Rv
D)
SBST05 133.3±9.1 Ma
34.05277N
76.77240E
SBST12 Leucogabbro 135.9±1.2 Ma
34.0625N; 76.7821E
Pegmatitic
gabbro veins
Massive gabbro sheets
within peridotite
E)
Photang thrust sheet
Permian OIB seamount
SP05 Gabbro ~135 Ma
34.0625N; 76.7821E

Figure 3

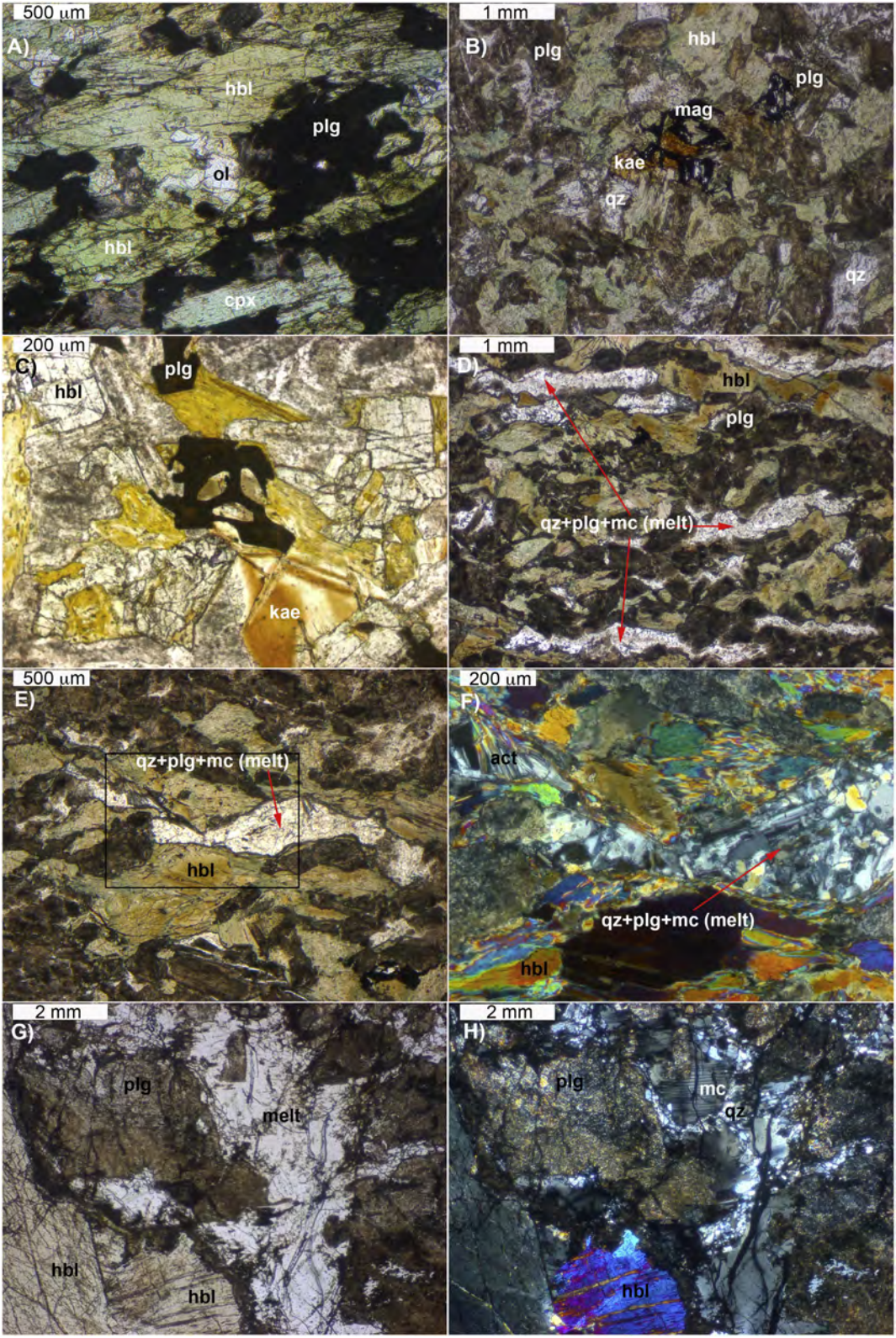
500 µm
A)
hbl
plg
ol
hbl
cpx
1 mm
B)
plg
hbl
plg
mag
kae
qz
qz
200 µm
C)
hbl
plg
kae
1 mm
D)
hbl
plg
qz+plg+mc (melt)
500 µm
E)
qz+plg+mc (melt)
hbl
200 µm
F)
act
qz+plg+mc (melt)
hbl
2 mm
G)
plg
melt
hbl
hbl
2 mm
H)
plg
mc
qz
hbl

Figure 4

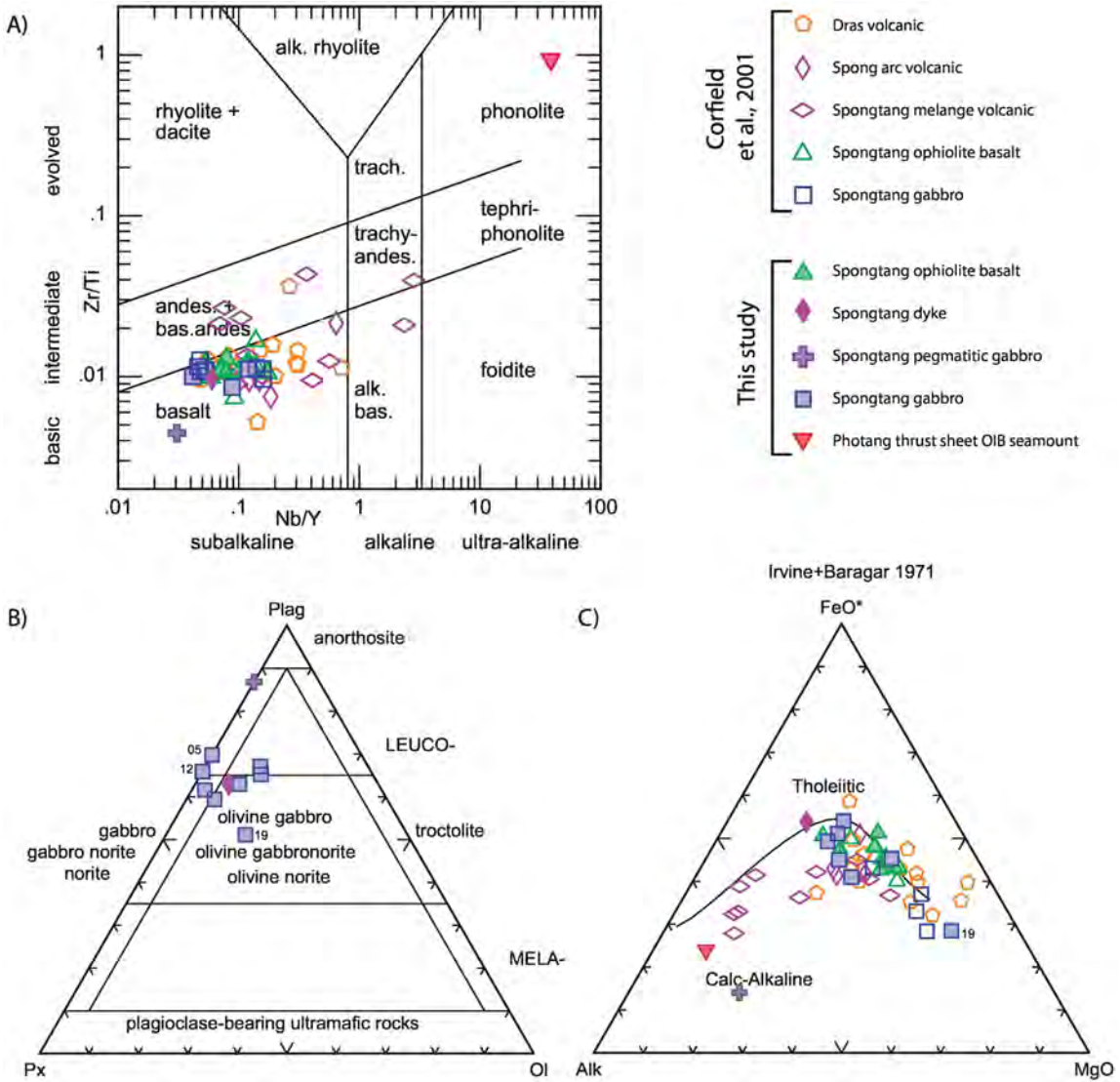
A)
alk. rhyolite
rhyolite +
dacite
phonolite
trach.
tephri-
phonolite
trachy-
andes.
andes. +
bas.andes
foidite
alk.
bas.
basalt
evolved
intermediate
basic
Zr/Ti
1
.1
.01
.01
.1
1
10
100
Nb/Y
subalkaline
alkaline
ultra-alkaline
Corfield
et al., 2001
Dras volcanic
Spong arc volcanic
Spongtang melange volcanic
Spongtang ophiolite basalt
Spongtang gabbro
This study
Spongtang ophiolite basalt
Spongtang dyke
Spongtang pegmatitic gabbro
Spongtang gabbro
Photang thrust sheet OIB seamount
B)
Plag
anorthosite
LEUCO-
troctolite
MELA-
gabbro
gabbro norite
norite
olivine gabbro
olivine gabbronorite
olivine norite
05
12
19
plagioclase-bearing ultramafic rocks
Px
Ol
C)
Irvine+Baragar 1971
FeO*
Tholeiitic
Calc-Alkaline
19
Alk
MgO

Figure 5

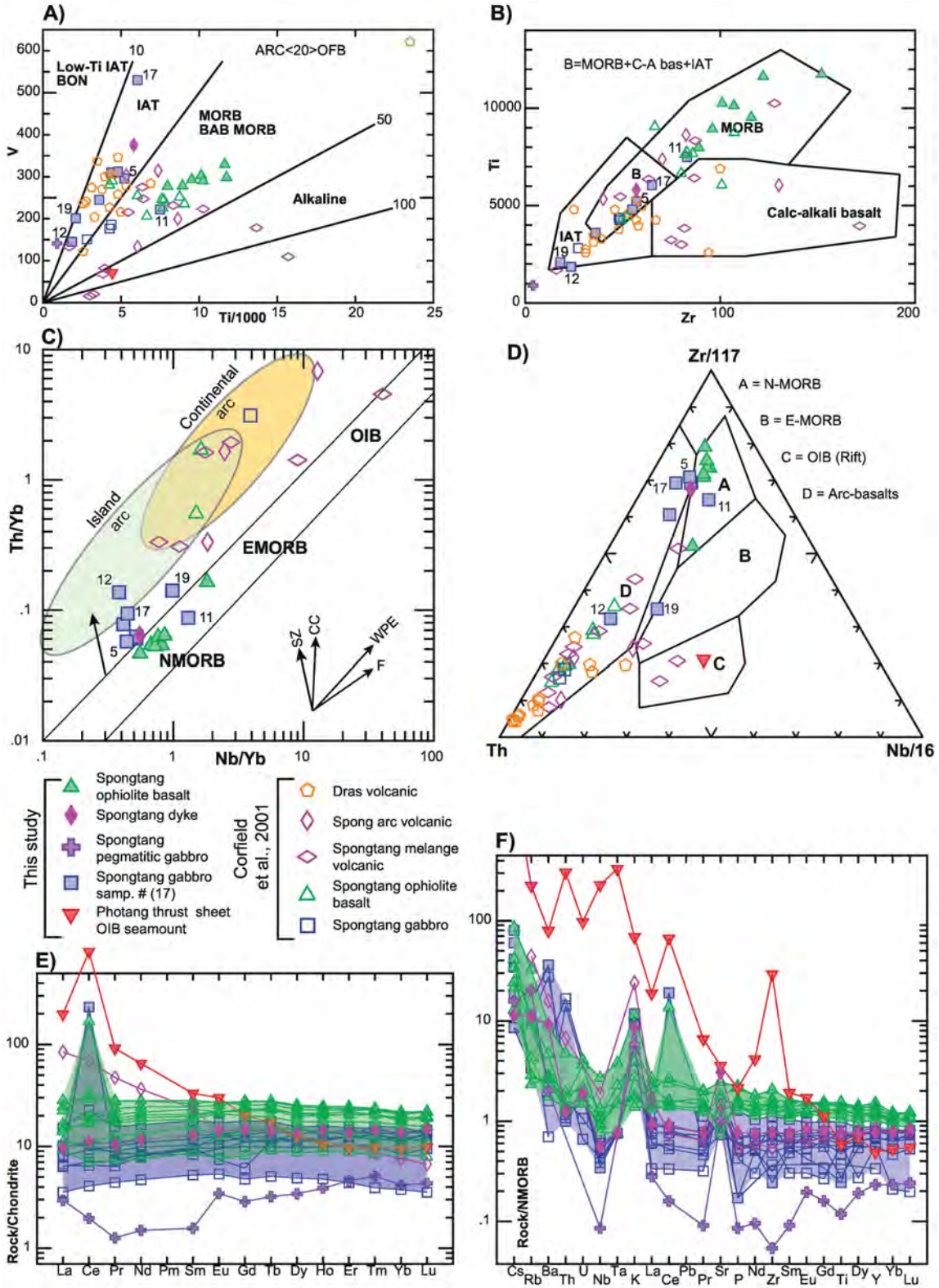
A)
Low-Ti IAT
BON
IAT
MORB
BAB MORB
Alkaline
ARC<20>OFB
V
Ti/1000
B)
B=MORB+C-A bas+IAT
MORB
Calc-alkali basalt
IAT
Ti
Zr
C)
Continental arc
Island arc
OIB
EMORB
NMORB
Th/Yb
Nb/Yb
D)
Zr/117
A = N-MORB
B = E-MORB
C = OIB (Rift)
D = Arc-basalts
Th
Nb/16
This study
Spongtang ophiolite basalt
Spongtang dyke
Spongtang pegmatitic gabbro
Spongtang gabbro samp. # (17)
Photang thrust sheet OIB seamount
Corfield et al., 2001
Dras volcanic
Spong arc volcanic
Spongtang melange volcanic
Spongtang ophiolite basalt
Spongtang gabbro
E)
Rock/Chondrite
La Ce Pr Nd Pm Sm Eu Gd Tb Dy Ho Er Tm Yb Lu
F)
Rock/NMORB
Cs Rb Ba Th U Nb Ta K La Ce Pb Pr Sr P Nd Zr Sm Eu Gd Ti Dy Y Yb Lu

Figure 6

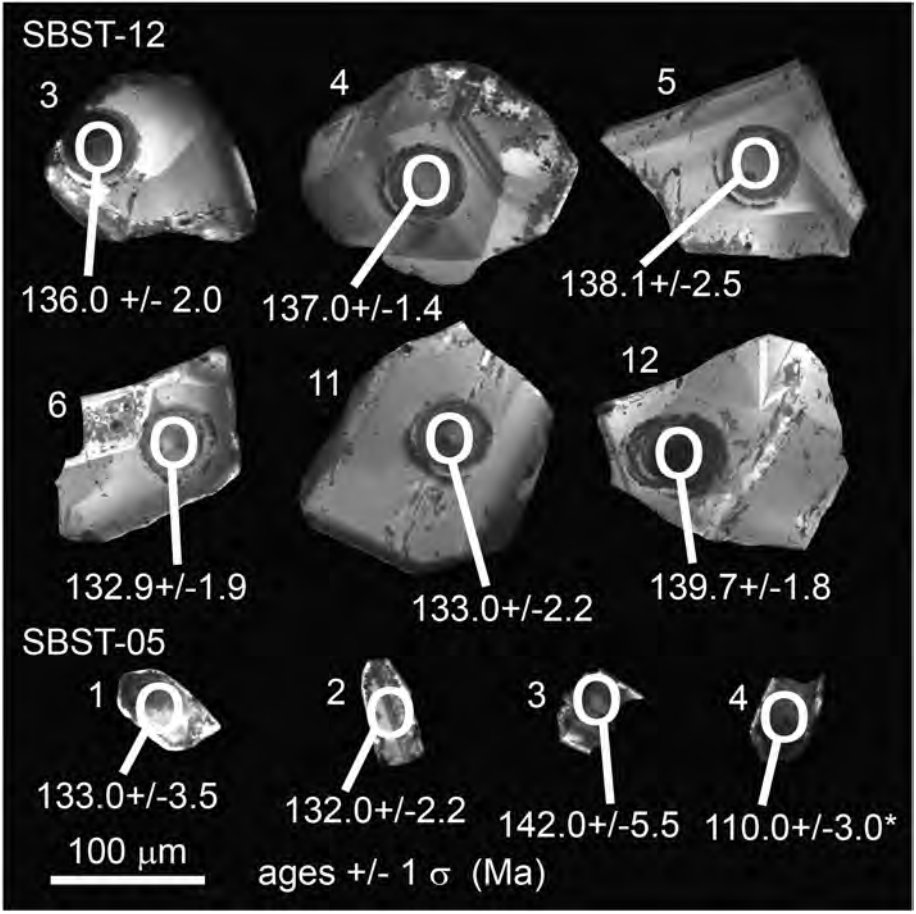
SBST-12
3
136.0 +/- 2.0
4
137.0+/-1.4
5
138.1+/-2.5
6
132.9+/-1.9
11
133.0+/-2.2
12
139.7+/-1.8
SBST-05
1
133.0+/-3.5
2
132.0+/-2.2
3
142.0+/-5.5
4
110.0+/-3.0*
100 μm
ages +/- 1 σ (Ma)

Figure 7

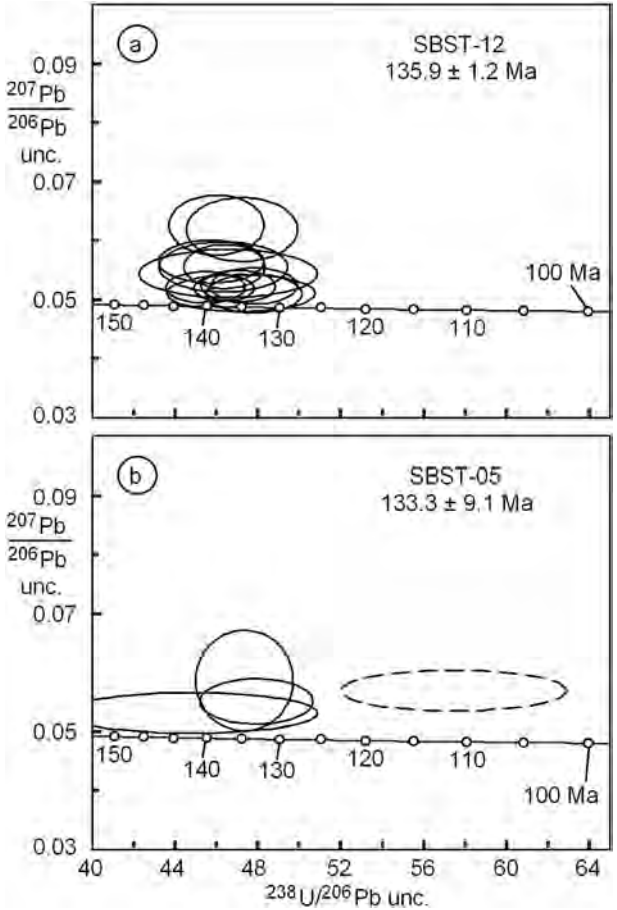
a
SBST-12
135.9 ± 1.2 Ma
0.09
207Pb/206Pb unc.
0.07
0.05
0.03
150
140
130
120
110
100 Ma
b
SBST-05
133.3 ± 9.1 Ma
0.09
207Pb/206Pb unc.
0.07
0.05
0.03
150
140
130
120
110
100 Ma
40
44
48
52
56
60
64
238U/206Pb unc.

Figure 8

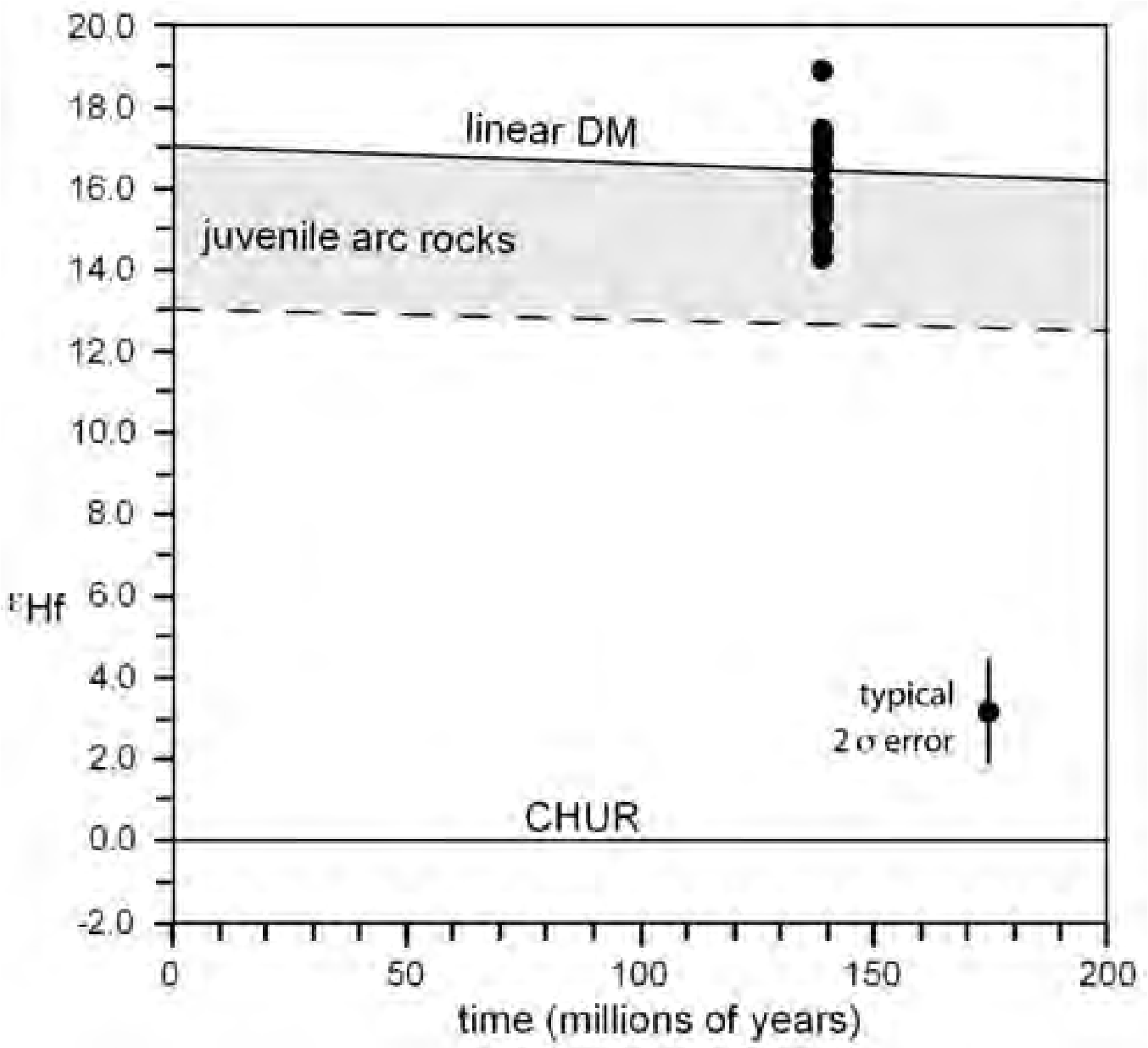
20.0
18.0
16.0
14.0
12.0
10.0
8.0
6.0
4.0
2.0
0.0
-2.0
εHf
linear DM
juvenile arc rocks
typical
2 σ error
CHUR
0
50
100
150
200
time (millions of years)

Figure 9

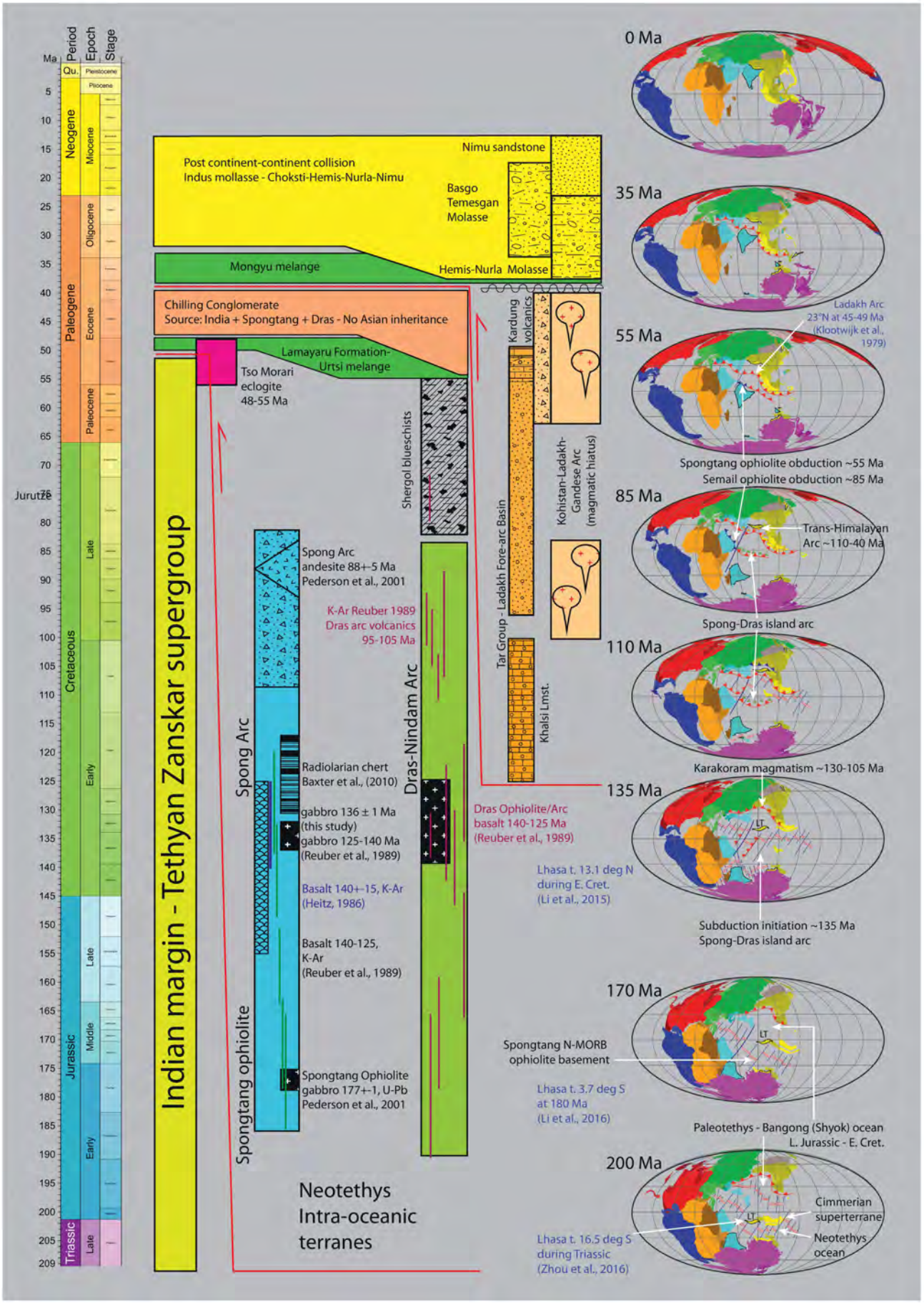
Ma
Period
Epoch
Stage
Qu.
Pleistocene
Pliocene
Neogene
Miocene
Oligocene
Paleogene
Eocene
Paleocene
Late
Early
Cretaceous
Jurassic
Middle
Triassic
Jurutze
Post continent-continent collision
Indus mollasse - Choksti-Hemis-Nurla-Nimu
Nimu sandstone
Basgo
Temesgan
Molasse
Hemis-Nurla Molasse
Mongyu melange
Chilling Conglomerate
Source: India + Spongtang + Dras - No Asian inheritance
Lamayaru Formation-
Urtsi melange
Tso Morari
eclogite
48-55 Ma
Indian margin - Tethyan Zanskar supergroup
Shergol blueschists
Kardung volcanics
Kohistan-Ladakh-
Gandese Arc
(magmatic hiatus)
Tar Group - Ladakh Fore-arc Basin
Khalsi Lmst.
Spong Arc
andesite 88+-5 Ma
Pederson et al., 2001
K-Ar Reuber 1989
Dras arc volcanics
95-105 Ma
Dras-Nindam Arc
Spong Arc
Radiolarian chert
Baxter et al., (2010)
gabbro 136 ± 1 Ma
(this study)
gabbro 125-140 Ma
(Reuber et al., 1989)
Basalt 140+-15, K-Ar
(Heitz, 1986)
Basalt 140-125,
K-Ar
(Reuber et al., 1989)
Spongtang ophiolite
Spongtang Ophiolite
gabbro 177+-1, U-Pb
Pederson et al., 2001
Dras Ophiolite/Arc
basalt 140-125 Ma
(Reuber et al., 1989)
Neotethys
Intra-oceanic
terranes
0 Ma
35 Ma
55 Ma
Ladakh Arc
23°N at 45-49 Ma
(Klootwijk et al.,
1979)
Spongtang ophiolite obduction ~55 Ma
Semail ophiolite obduction ~85 Ma
85 Ma
Trans-Himalayan
Arc ~110-40 Ma
Spong-Dras island arc
110 Ma
Karakoram magmatism ~130-105 Ma
135 Ma
LT
Lhasa t. 13.1 deg N
during E. Cret.
(Li et al., 2015)
Subduction initiation ~135 Ma
Spong-Dras island arc
170 Ma
LT
Spongtang N-MORB
ophiolite basement
Lhasa t. 3.7 deg S
at 180 Ma
(Li et al., 2016)
Paleotethys - Bangong (Shyok) ocean
L. Jurassic - E. Cret.
200 Ma
LT
Cimmerian
superterrane
Neotethys
ocean
Lhasa t. 16.5 deg S
during Triassic
(Zhou et al., 2016)

Figure 10

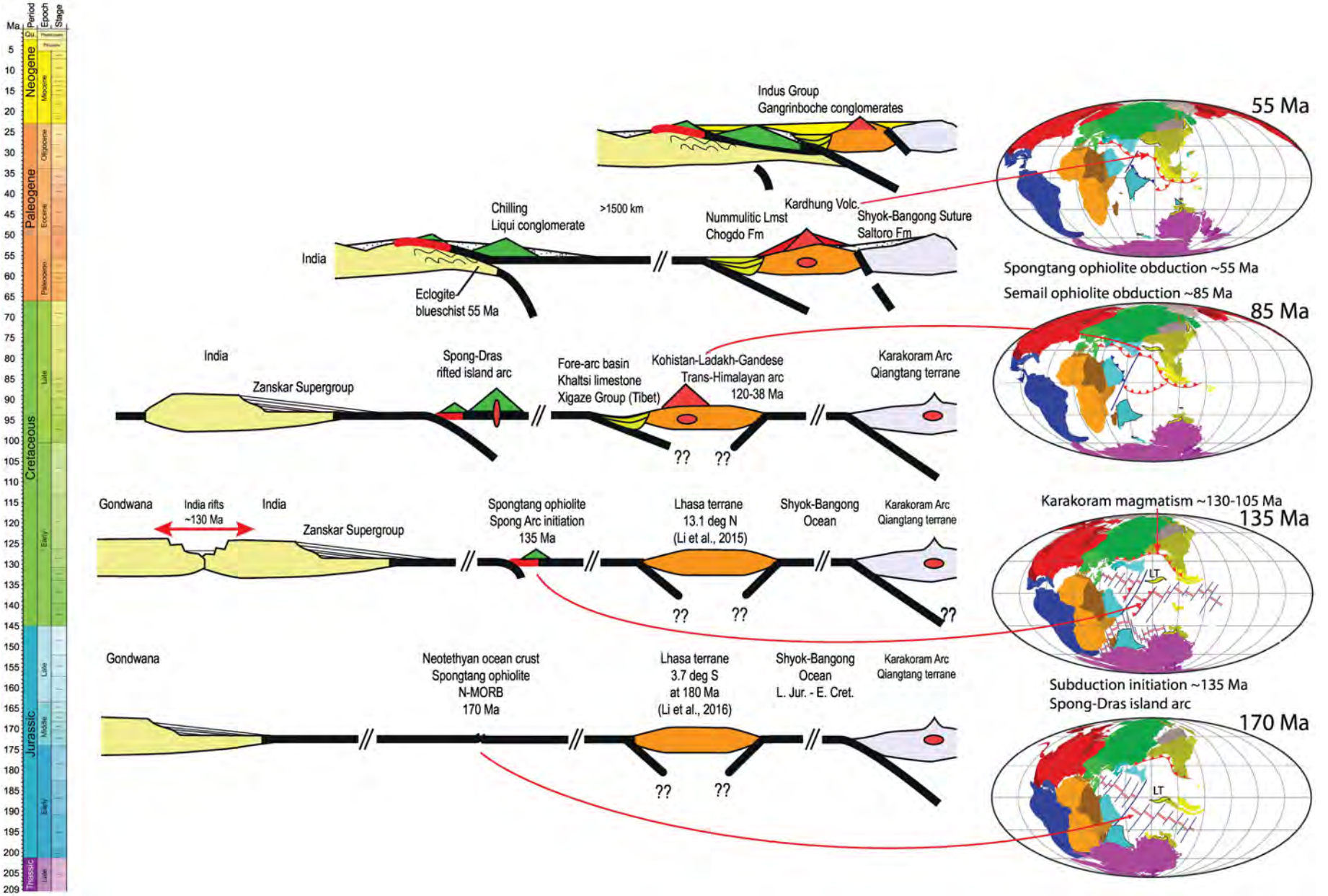
Ma
Period
Epoch
Stage
Neogene
Paleogene
Cretaceous
Jurassic
Triassic
Indus Group
Gangrinboche conglomerates
Chilling
Liqui conglomerate
>1500 km
Kardhung Volc.
Nummulitic Lmst
Chogdo Fm
Shyok-Bangong Suture
Saltoro Fm
India
Eclogite
blueschist 55 Ma
55 Ma
Spongtang ophiolite obduction ~55 Ma
Semail ophiolite obduction ~85 Ma
85 Ma
India
Zanskar Supergroup
Spong-Dras
rifted island arc
Fore-arc basin
Khaltsi limestone
Xigaze Group (Tibet)
Kohistan-Ladakh-Gandese
Trans-Himalayan arc
120-38 Ma
Karakoram Arc
Qiangtang terrane
??
??
Karakoram magmatism ~130-105 Ma
135 Ma
Gondwana
India rifts
~130 Ma
India
Zanskar Supergroup
Spongtang ophiolite
Spong Arc initiation
135 Ma
Lhasa terrane
13.1 deg N
(Li et al., 2015)
Shyok-Bangong
Ocean
Karakoram Arc
Qiangtang terrane
LT
Subduction initiation ~135 Ma
Spong-Dras island arc
170 Ma
Gondwana
Neotethyan ocean crust
Spongtang ophiolite
N-MORB
170 Ma
Lhasa terrane
3.7 deg S
at 180 Ma
(Li et al., 2016)
Shyok-Bangong
Ocean
L. Jur. - E. Cret.
Karakoram Arc
Qiangtang terrane
LT

Figure 11